KGHM

Ajax Pit Lake Model Report

Project No. J933-4

12 August 2015

LORAX ENVIRONMENTAL

2289 Burrard Street
Vancouver, BC, V6J 3H9
Canada

Disclaimer

KGHM

Disclaimer

This document has been prepared by Lorax Environmental Services Ltd. ("Lorax") for the benefit of the client named in this document. Lorax has no liability, obligation or responsibility for any changes to this document or any of its contents made by any person other than Lorax or its authorized personnel.

Table of Contents

KGHM

Table of Contents

LIST OF FIGURES

LIST OF TABLES

List of Acronyms

List of Acronyms

TDS	Total Dissolved Solids
NCEP	National Centres for Environmental Protection
CFSV2	Climate Forecast System Version 2
CFSR	Climate Forecast System Reanalysis
GCM	General Circulation Model
FLNRO	British Columbia Ministry of Forests, Lands and Natural Resource Operations
EC	Environment Canada
KP	Knight Piesold Ltd
BGC	BGC Engineering
MRSF	Mine Rock Storage Facility
TSF	Tailings Storage Facility
IMH	Iron Mask Hybrid
SLD	Sugarloaf Diorite
SLVHB	Sugarloaf Volcanic Hybrid
PICR	Picrite
MAFV	Mafic Volcanics
DO	Dissolved Oxygen
OM	Organic Matter
PET	Potential Evapotranspiration
LOM	Life of Mine
PAG	Potentially acid generating
NPAG	Non Potentially acid generating
NP	Neutralization potential

Glossary

Glossary

Albedo	Fraction of solar energy reflected back into space from earth’s surface
Anoxic	Areas of pit lake water depleted of oxygen or less than 0.5 mg/L
Black Body	Refers to a system which absorbs all incident radiation and emits radiation which is characteristic of the system.
Chemocline	Chemistry based transition layer between mixed surface layer and deep water layer
Downward Longwave Radiation	Longwave radiation reflected back to earth's surface from the atmosphere
Downward Shortwave Radiation	Total solar irradiance incident at the Earth's surface
Empirical	Is a source of knowledge acquired by observation and experimentation
Epilimnion	Upper water layer in stratified lake
Eutrophic	Refers to waters rich in phosphates, nitrates, and organic nutrients that are able to promote and sustain plant life.
Halocline	Salinity based transition layer between mixed surface layer and deep water layer
Hypolimnion	Deep water layer in stratified lake
Hypsographic	Scientific description of topographic properties of open pits typically plotted as curves of elevation versus storage volume and elevation versus planar area
Latent Heat	Type of energy released or absorbed in the atmosphere and is related to changes in phase between liquids, gases, and solids.
Meromictic	Refers to a vertically stratified lake with layers that do not intermix.
Morphometry	Quantitative measurement of open pit shape
Oligotrophic	Environments offering very low levels of nutrients
Pycnocline	Density based transition layer between mixed surface layer and deep water layer

Redox	Refers to chemical reactions involving transfer of electrons between species
Sensible Heat	Type of energy released or absorbed in the atmosphere and is related to changes in temperature of a gas or object with no change in phase.
Thermocline	Temperature based transition layer between mixed surface layer and deep water layer

1. Introduction

KGHM

1. Introduction

1.1 Overview

KGHM Ajax Inc. (KAM) is applying for an Environmental Assessment Certificate for the Ajax Project. The Project includes the development of an open pit mine located south of Kamloops in south central British Columbia. Mining of the pit will result in the development of a pit void at final closure with a maximum volume of ~410 Mm^3 and a horizontal planar surface area of ~217 ha.

KAM retained Lorax Environmental Services Ltd. (Lorax) to conduct a pit lake modelling study for the lake that will form in the pit void. The pit lake model incorporates input parameters from baseline monitoring and from other models including the pit wall geochemical loading terms from each geologic unit on the pit wall, water balance and water quality models. This report includes a discussion of these various input parameters.

Lorax has utilized the one-dimensional coupled hydrodynamic-geochemical model PitMod to predict the evolution in the water column of temperature, salinity, density, and concentrations for a host of geochemical parameters. PitMod is a one-dimensional hydrodynamic model used for predicting the spatial and temporal distribution of temperature, density, dissolved oxygen and water quality in lakes (Crusius and Dunbar, 2000). The one-dimensional approximation is particularly applicable to pit lakes due to their high depth to surface area ratio and the fact that there are few, if any, barriers to horizontal mixing relative to those observed in the vertical dimension (*e.g.*, thermoclines and haloclines). Model results provide information on the chemistry of water layers with depth and time in the pit lake. The results of the pit lake model are presented in this report along with the implications of these results regarding water management at the site.

1.2 Approach and Objectives

Pit lake modelling was conducted for the purpose of determining and assessing predicted long term pit lake water quality for the Ajax open pit. The general study approach was to construct the pit lake model using inputs from the pit wall loading estimates and water balance and water quality models that were prepared by other consultants working on the Ajax project. The primary objective of this study is the construction of a pit lake model that provides an understanding of how the pit lake water quality will evolve during the post-closure period.

Upon completion of the 2014 baseline data collection and compilation, final water balance models and water quality models were prepared for KAM and the results of these models were provided to Lorax.

2. Approach and Methodology

KGHM

2. Approach and Methodology

2.1 Lake Physics

Water quality in the Ajax pit lake will depend primarily on the vertical distribution of dissolved solids concentrations and dissolved oxygen as the pit shell fills with surface and groundwater inflows. The concentration of total dissolved solids (TDS) together with water temperature will determine the water density at any depth in the lake. Water density increases with increasing TDS while the relationship between water density and water temperature is more complex. In the Ajax model water density is calculated using an empirical equation of state together with values for both temperature and TDS. Therefore, the values of TDS and temperature are sufficient to predict the density structure, stability, and mixing properties in the lake as it fills.

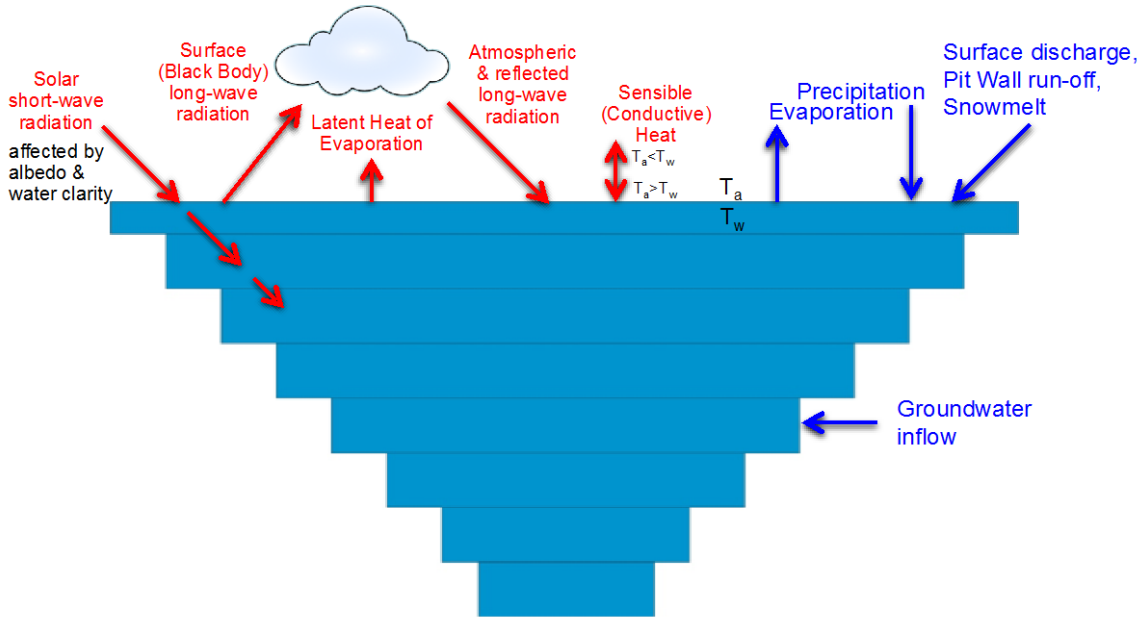

Figure 2-1: Components of the heat (red) and mass (blue) balances in the Ajax pit lake

Temperature and TDS in the Ajax pit lake will depend on the heat and mass balances depicted in Figure 2-1. Components of the heat balance are shown in red, while components of the mass balance are shown in blue. Water and solids will be added to the lake via precipitation and snowmelt, surface inflows from various sources, pit wall runoff, and groundwater inflow - both above and below the lake surface. Temperature changes in the lake will occur due to the heat content of the various inflows, heat added from incoming solar long- and short-wave radiation (*i.e.*, infrared and ultraviolet), heat loss due to out-

going long-wave black body radiation at the lake surface (and possibly reflected back to the surface from clouds), sensible heat exchange between the air (or ice) and the lake surface, and the loss of heat due to evaporation. Each of these sources and sinks for mass and heat are included in the Ajax model. Some, such as heat loss due to evaporation, are relatively complex and depend on other properties such as wind speed, relative humidity, and air and water temperatures.

The depth and dimensions of the Ajax pit will have a strong effect on water quality and density structure in the lake as it evolves. Pit lakes, in contrast to most natural lakes, are relatively deep and steep-sided, with large values for relative depth Z_r – the ratio of maximum depth to mean surface diameter (Gammons and Duaime, 2006). The relatively small surface diameter of many pit lakes in comparison with their maximum depth results in a less effective transfer of wind energy from the surface to deeper waters, thereby limiting vertical mixing. Most natural lakes at temperate latitudes are characterized by Z_r values of <2% and undergo seasonal turnover. Studies of naturally occurring meromictic lakes in North America show Z_r values of >5% (Anderson *et al*., 1985). Due to the morphometry of open pits, pit lake systems show much higher Z_r, with values generally ranging from 10 to 40%, indicating a greater tendency for permanent stratification. At the end of the 200-year model simulation, the Ajax pit lake is predicted to have a maximum depth of 289 m and a surface area of 95 ha. At this time the lake would have a Z_r value of 26% and exhibit a propensity for stratification.

The large relative depth of the Ajax pit lake has important implications for the downward penetration of thermal and wind energy, and their concomitant effects on vertical mixing and stability. Unlike natural lakes, which often have a layer of organic matter at the bottom, the bottom of a pit lake initially consists of bare, oxidized rock. In addition, pit lakes often receive inflowing waters with high TDS values which impact density.

Density in freshwater lakes is largely determined by temperature and to a lesser extent by the TDS concentration, or salinity (Figure 2-2). The density of pure liquid water attains a maximum of 0.99998 g/cm^3 at 3.94°C. Therefore, dense natural lake bottom waters tend to remain near 4°C while the temperature near the surface varies in response to inflows and changing atmospheric conditions.

The addition of dissolved salts to freshwater results in an increase in density. Seawater, for example, has a density 2.8% greater than freshwater. The Ajax pit lake will receive water that has a wide range of dissolved salts and other geochemical species due to inflows of groundwater, precipitation, and other surface inflows contacting exposed pit wall surfaces. At the end of the 200-year model simulation the water density at the bottom of

the Ajax lake is predicted to be 1006.5 kg/m^3 which is significantly greater than freshwater, while the surface waters will be only slightly denser than freshwater at 1001.8 kg/m^3.

The density of pit lake water is determined by applying an empirical equation of state relating water temperature and salinity to water density. Salinity can be accurately determined by measuring the conductivity of the water. The equation of state for water is nonlinear with temperature for a fixed conductivity, and nearly linear with conductivity for a fixed temperature (Figure 2-2).

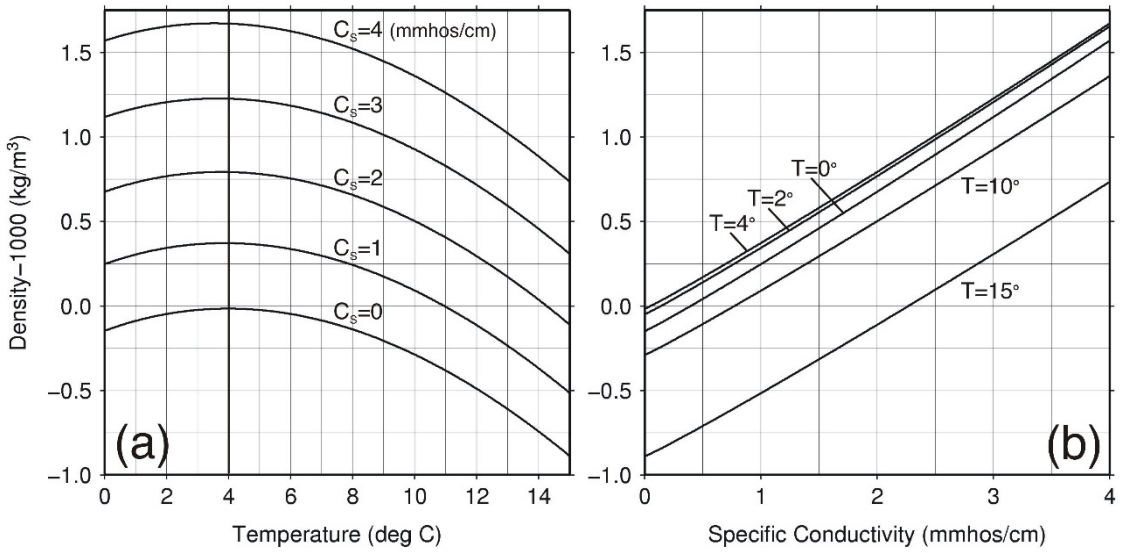

Figure 2-2: Water density for different values of (a) specific conductivity (a measure of TDS), and (b) temperature.

Deep, freshwater lakes typically have at least two layers: a bottom hypolimnion, whose waters are at least seasonally isolated from the atmosphere (and sometimes perennially stagnant), and an upper epilimnion that is well mixed by the wind. The two layers are separated by a relatively thin region marked by a strong density gradient (pycnocline).

The physical stability of a stratified lake can be described by the tendency for the upper and lower water layers to mix. The energy required to completely mix two water masses of differing density increases with the density difference. Specifically, given two layers of density ρ_1 and ρ_2, and of equal volume and thickness *h*, the energy, ΔE, required to mix the two volumes completely, ignoring viscous dissipation of energy, is for small $\Delta\rho = \rho_2 - \rho_1$:

$$\Delta E = \frac{gh\Delta\rho}{2}.$$

This is the energy required to raise the centre of mass of the original two layers to their geometric centre. A large difference in density across a strong density gradient (pycnocline) suppresses mixing and increases the vertical stability of the water column.

Both natural and pit lakes at high latitudes experience regular, seasonal ice formation, with the timing and duration of the ice cover dependent primarily on latitude and altitude, but also on inter-annual variability of air temperature, wind velocity, and solar radiation.

A period of ice cover, and the changes in lake temperature that precede and follow it, profoundly affect the physical properties of lakes. From thermally stratified conditions in late summer, lake surface waters cool and increase in density as autumn approaches until a temperature of approximately 4° C is reached, at which point maximum density is attained and the lake convectively mixes. The degree of mixing depends on the lake depth and vertical density gradient. Some lakes mix fully every year, while others may mix fully only occasionally. Meromixis occurs when complete mixing is inhibited due to high bottom layer solute concentrations, at which time mixing is limited to only the upper layers of the lake.

If the temperature decreases sufficiently, ice will begin to form, thickening over the winter months. The lake will again become thermally stratified, with less dense 0° C water in a surface layer overlying warmer, denser water below.

The ice thermally insulates surface waters from the cooler air above and eliminates wind mixing. Snow accumulates on the ice, storing water until it thaws with the arrival of warmer temperatures. With the formation of ice, the level of the lake will drop if surface inflows decrease or stop altogether. Some solutes may become supersaturated immediately under the ice due to salt expulsion as the ice forms.

During the subsequent spring and summer thaw, the snow and ice melt and their volumes are added to the lake over a relatively short interval together with runoff from the surrounding watershed. This sudden influx of water (freshet) may represent a significant portion of the annual surface water budget.

As the ice and snow melt and surface waters warm to temperatures above 0° C the water density increases as the temperature increases toward 4° C leading to convective mixing and overturning in many natural lakes. The twice-annual cycle of fall-winter and spring-summer overturning is the defining characteristic of dimictic lakes. Thus, it is important to include ice formation and thawing in models of pit lakes where this occurs due to their impact on lake dynamics (Patterson and Hamblin, 1988; Rogers, Lawrence *et al*., 1995; Hamblin, Stevens *et al.*, 1999).

2.2 Geology

The Ajax pit is located on the southwest side of the Iron Mask batholith, at the contact between medium to coarse grained Iron Mask hybrid diorite and Sugarloaf diorite. The geology of the pit wall is an important consideration when assessing the evolution of the pit lake water chemistry, due to the unique acid generating potential and leaching characteristics of each rock type and the relative area of exposure on the pit wall. This section describes the geology of the major rock units; the leaching characteristics of these units is described subsequently in Chapter 3.

There are five major rock units included in the Ajax pit lake model:

1. Iron Mask Hybrid – IMH
2. Sugarloaf Diorite – SLD
3. Sugarloaf Volcanic Hybrid – SLVHB
4. Mafic Volcanics – MAFV
5. Picrite – PICR

Each of these rock units are discussed in the following sections that provide a brief description of their genesis and mineral composition.

2.2.1 Iron Mask Hybrid

The Iron Mask hybrid unit is thought to represent the assimilation of Nicola Volcanic rocks into the intruding Pothook diorite (Logan and Mihalynuk, 2006). Compositionally, it is dioritic to gabbroic. The rock may contain up to 10% magnetite and is strongly magnetic. The unit is typically unmineralized but can contain localized pyrite and chalcopyrite, especially near the contact with Sugarloaf units.

2.2.2 Sugarloaf Diorite (and Sugarloaf Volcanic Hybrid)

The Sugarloaf Diorite unit is commonly a fine-grained porphyritic hornblende diorite located along the contact between the Nicola Group volcanics and the Iron Mask hybrid (Logan and Mihalynuk, 2006). The Sugarloaf diorite is the main host to copper-gold mineralization in the Ajax deposit. Where unaltered, the rock may contain up to 5% fine, anhedral magnetite.

The Sugarloaf diorite may show strong albite alteration, obliterating original textures. Albite alteration shows variable intensity and is common near zones of mineralization within the unit. Sulphide mineralization, may consist of 1 to 10% combined pyrite and chalcopyrite with minor molybdenite (MoS_2), rare tetrahedrite ($Cu_{12}Sb_4S_{13}$) and bornite. Up to 3% irregular calcite veins may be present locally.

Where Sugarloaf diorite has partially assimilated blocks of mafic (Nicola) volcanics a heterogeneous, mixed rock has resulted. This rock is generally referred to as the Sugarloaf Volcanic Hybrid. It has a similar alteration and mineralization assemblage to that of the Sugarloaf diorite.

2.2.3 Mafic Volcanics

A thick sequence of Nicola Group Mafic Volcanic rocks lies to the south of and structurally below the Sugarloaf Diorite within the ultimate Ajax open pit. These rocks are described as basaltic to andesitic flows and flow breccias, light green massive tuffs and bedded ash to lapilli tuffs. The unit is medium to dark green and non to weakly magnetic.

2.2.4 Picrite

The Picrite occurs as wedges or slivers caught up in major fault-related northwest trending, northeast dipping structural corridors within the Iron Mask batholith and are believed to have been emplaced into the Nicola Group Volcanics. The Picrite is generally dark green in colour, fine-grained and strongly magnetic and may contain up to 10% olivine phenocrysts, now altered to serpentine and magnetite. The matrix generally consists of serpentine and tremolite-actinolite. Minor (<1 %) chalcopyrite and pyrite may occur locally, typically near the contacts with Sugarloaf Diorite and Sugarloaf Volcanic Hybrid, but the Picrite is generally unmineralized. The rock may be cut by up to 3% irregular calcite veins and fractures within the unit are often infilled with talc.

2.3 Overview of Pit Lake Physics and Geochemical Processes

The density structure of stratified lakes has an important influence on the chemical and biological processes that occur in both the water column and sediments. In particular, the restricted mixing across the pycnocline can result in the depletion of O_2 and the accumulation of other chemical species associated with the breakdown of organic matter in the bottom of the lake. In natural aquatic systems, dissolved oxygen is consumed principally by bacterially-mediated oxidation of organic matter (OM) (Fenchel and Blackburn, 1979; Stumm and Morgan, 1981). OM produced in the surface waters (*i.e.*, plankton, zooplankton, *etc.*) is delivered to the interior of the lake and lake bottom via the settling of organic detritus.

Due to the downward transport of OM, the oxidation reactions associated with its degradation occur throughout the water column. Organic matter is oxidized or remineralized by both aerobic and anaerobic bacteria. These remineralization reactions are redox processes in which electrons are transferred from the reductant (OM) to an electron acceptor (oxidant). In shallow lakes, much of the oxidation of OM occurs at the sediment-

water interface, while in deeper lakes significant OM oxidation can occur in bottom water (Northcote and Johnson, 1964; Hamilton-Taylor and Davison, 1995). Collectively, these oxidation processes result in depletion of oxygen in the bottom waters. Without deep water mixing and associated replenishment of oxygen, or where the OM flux to bottom waters is high (as in productive or eutrophic lakes), oxygen-consuming reactions can result in the complete depletion of oxygen (anoxia) in bottom waters.

In aerobic environments, oxygen is preferentially used as the final electron acceptor in the oxidation of OM. Once oxygen is depleted, other electron acceptors are employed. Based on decreasing free energy yield, thermodynamics dictates that electron acceptors are used in the order: $O_2 > NO_3^- \approx Mn^{IV}$-oxides > Fe^{III}-oxides > SO_4^{2-} (Froelich, Klinkhammer *et al.* 1979; Stumm and Morgan 1981; Sigg, Johnson *et al.* 1991). Once oxygen has been exhausted as an oxidant, nitrate will be employed as the electron acceptor for OM oxidation, followed by Mn-oxides, *etc*.

The development of anoxic bottom waters can greatly influence the behavior of trace elements. Of particular importance is the reduction of sulfate, which liberates hydrogen sulfide (H_2S). In most mine pit lake scenarios, sulfate is readily available and at concentrations capable of generating significant quantities of hydrogen sulfide. Many trace elements (*e.g.*, Fe, Co, Ni, Zn, Cd, and Pb) react rapidly with free sulfide to precipitate insoluble sulfide minerals (Stumm and Morgan 1981; Balistrieri, Murray *et al*. 1994). Consequently, the precipitation of metal sulfides and their subsequent settling to the lake floor can provide an effective mechanism for removing trace elements from the water column (Green, Ferdelman *et al*. 1989; Achterberg, van den Berg *et al.* 1997).

Except for dissolved Oxygen (DO), the concentrations of all chemical species in the Ajax model simulation are initially determined by applying a conservative volume weighted mixing scheme. For example, in the case of the complete mixing of a solute in two adjacent layers of the model—the process used in convective mixing—the concentration after mixing is calculated using

$$C_i' \equiv C_{i+1}' = \frac{V_i C_i + V_{i+1} C_{i+1}}{V_i + V_{i+1}},$$

where V_i and C_i are the volume and concentration, respectively, in layer *i*.

In the case of DO an additional calculation is used to simulate the removal of oxygen from *in situ* demand. Using data from Charlton (1980) a value of 510 mg m^{-2} day^{-1} for hypolimnion oxygen consumption appropriate for an oligotrophic lake was used in the Ajax model, which is consistent with the range of values reported by Müller *et al*, 2012. This DO consumption rate per unit surface area is converted to a rate per unit volume by

dividing 510 mg m^{-2} day^{-1} by a length scale equal to the pit lake volume divided by the surface area.

2.4 Description of Ajax Pit Lake Model

PitMod is a proprietary, one-dimensional numerical model developed by Lorax Environmental Services (Crusius *et al*. 2002; Dunbar *et al*., 2004). It is specifically designed to model the evolution and vertical distribution of physical and geochemical properties of pit lakes over long time periods. PitMod incorporates physical processes similar to those in other lake models such as DYRESM (Imerito, 2007). However, unlike DYRESM, PitMod also includes geochemical processes via coupling to the PHREEQC speciation model, the effects of surface ice formation, and geochemical and physical processes unique to pit lakes.

The one-dimensional approximation used by PitMod is appropriate for pit lakes due to their generally greater relative depth than found in most natural lakes, and the absence of barriers to horizontal mixing. Model outputs include the temporal distribution of lake elevation and volume, and vertical and temporal distributions of temperature, salinity, density, pH, and a suite of geochemical species concentrations.

PitMod may be run in either non-conservative or conservative modes. In the former, PitMod uses PHREEQC to determine equilibrium concentrations of geochemical species that result from mixing two geochemically distinct water volumes together. In the latter, calls to PHREEQC are omitted, and geochemical concentrations of mixed solutions are determined from simple mass and volume conservation equations.

Implementation of a non-conservative PitMod model is most applicable when large proportions of acidic and alkaline waters are mixed, which often leads to the precipitation of secondary iron (Fe) and manganese (Mn) hydroxide minerals and calcium/magnesium carbonate minerals that may incorporate metals into their crystal structure, effectively removing the dissolved metal constituents from solution. The Ajax PitMod simulation was completed in conservative mode to predict physical and geochemical pit lake properties from the start of pit filling through the subsequent 200 years. Conservative mode provides a reasonable approach for modelling the surface water chemistry of the Ajax pit lake due to similar pH for the various water sources that mix in the pit lake. The effect of secondary mineral controls is largely accounted for by the input water chemistry. Although reasonable, the implementation of PitMod in conservative mode over estimates metal cation concentrations as it does not account for scavenging and particle settling mechanisms that are common in natural lakes. These mechanisms have the greatest impact on the predicted Fe concentrations in an oligotrophic pit lake but would also reduce other metal concentrations including Cu, Co, Mn, Pb, Ni and Zn.

PitMod was selected to model the Ajax pit lake primarily because it is the only available model that can be easily tailored to accommodate site-specific physical and geochemical processes. Since PitMod was developed, and is actively maintained and enhanced by Lorax, it was possible to add the following capabilities specifically for the Ajax pit lake:

- Time-dependent surface mass loadings of pit wall geochemical species.
- Partitioning of groundwater inflows to above surface and below surface components, with the sub-surface components further divided into depth-dependent zones.
- Inclusion of water depth dependent groundwater inflow temperature.
- Time-series of monthly geochemical species concentrations for all source terms.
- The inclusion of depth-dependent backfill void volume that contributes to the capacity of the Ajax pit lake but does not participate in the lake mixing dynamics.
- Tailoring of surface ice formation and melting to agree with near-site observations.
- Pit wall geology comprised of geology types providing depth-dependent, surface area weighted run-off (*i.e.,* the contribution from each pit wall geology is proportional to its above-water surface area).

The physical processes simulated by PitMod determine the evolution of salinity, temperature, density (calculated from salinity and temperature), dissolved oxygen, and dissolved geochemical species in the water column. PitMod is 1-dimensional, with horizontal variations assumed to be negligible, and with the water column divided into a vertical stack of 1 m-thick homogeneous layers. The principal physical properties and processes included in PitMod that are used in the Ajax model are:

- *Pit Morphometry*: The effects of pit morphometry are included in the model by specifying the variation in pit shell volume and plan-view surface area with increasing elevation above the pit bottom to a level that includes the pit catchment area. This stage (or lake area) versus depth relationship determines the filling rate of the pit and strongly influences pit lake physical and geochemical properties.
- *Surface Heat Budget*: The Ajax pit lake temperature is determined in part by several processes that either add or remove heat energy within the near-surface layers of the pit lake, including: the absorption of long- and short-wave energy from the sun; surface heat loss due to outgoing long-wave black body radiation; the addition of long-wave radiation from cloud cover; evaporative cooling; and sensible, or conductive heat transfer. In addition, heat energy is transferred vertically via diffusion, wind mixing, and convection (discussed below).

- *Vertical mixing*: The kinetic energy of near-surface wind results in vertical mixing within the Ajax pit lake surface layer. The depth of the resulting wind-mixed layer depends on the energy flux from the wind, which is proportional to the cube of the wind speed, as well as the duration of the wind and the strength of the vertical density gradient (stratification) near the surface. The thickness of the wind-mixed layer decreases with increasing stratification.
- *Convection:* Convection in the Ajax model corresponds to vertical motion within the lake resulting from static instabilities in the water column that occur when changes in salinity and/or temperature within a layer increases its density above that of water in the underlying layer. This will result in instantaneous and complete mixing of any two such layers to restore a stable vertical density structure.
- *Oxygen Consumption*: Oxygen consumed in both the water column and sediments is an important variable in the geochemical state of the Ajax pit lake model. Oxygen is introduced to surface waters through interaction with the atmosphere and is distributed throughout the water column by mixing and diffusion across adjacent layers. Oxygen may also be introduced below the surface via groundwater inflows. The consumption of oxygen during organic matter degradation (*i.e.*, oxidation) may result in the development of anoxic conditions if the oxygen consumption rate exceeds its rate of replacement.
- *Addition / Removal of Water (Mass Balance)*: Water is added to the Ajax pit lake model at the surface and at various depths, and is removed via surface evaporation. This allows for the inclusion of complex sub-surface and surface groundwater inflow and precipitation and other surface inflows. The vertical distribution of groundwater inflow is specified using output data produced by the BGC groundwater model. Inflows have an associated temperature and water quality that determines its density. Removal of surface layer water through evaporation has the effect of concentrating solutes—and therefore increasing density—in the uppermost layer of the model (*i.e.*, evapo-concentration).
- *Pit Wall Runoff Effects*: The Ajax pit lake model includes mass source terms associated with precipitation and melting snow contacting exposed pit wall surfaces above the lake. Pit walls are partitioned into geology types, each having an associated cumulative surface area *versus* elevation distribution and geochemistry. PitMod determines the area of the pit wall above the lake surface for each geology type and then calculates the corresponding surface inflow when precipitation and melting snow contacts the pit walls and runs downward to the lake surface. A constant runoff coefficient of 0.65 is specified for each rock type.

- *Surface Geochemical Loading*: The Ajax pit lake model accommodates surface fluxes of stored geochemical species from the pit wall that are rinsed by the rising lake level but were not rinsed by runoff or precipitation. As the rising pit lake inundates fractured and broken rock on the pit wall, the stored geochemical loads from the freshly rinsed pit wall surfaces diffuse into the lake. In the Ajax model the stored mass per unit area increase linearly with time.
- *Surface Ice Formation and Snow Accumulation*: The Ajax pit lake model includes an algorithm for calculating the formation and thickness of surface ice and accumulated snowfall on the lake surface and on pit walls above the lake surface. It is based on the method of Rogers and Lawrence (1995). Ice sequesters water, lowering the lake level and suppresses surface wind-mixing. In addition, the model assumes that solutes in the water are excluded as ice is formed. This results in the increase in solute concentration in the topmost layer of the lake—with an effect similar to that of evapo-concentration.

The following assumptions are made to increase computational efficiency and to approximate complex physical processes:

- All properties in the flooded pit are horizontally homogeneous at all times; that is, they are functions of depth and time only;
- The effect of all water currents in the pit lake may be parameterized in a single vertical turbulent diffusion equation. Hence, the direct calculation of the velocity field in the flooded pit is omitted;
- The value of the vertical turbulent diffusion coefficient, which regulates the degree of vertical mixing of water properties, varies with depth and time, is solely a function of the local stratification and may be calculated directly from the static stability;
- Instabilities in the water column—that is, denser water overlying less dense water—are resolved immediately in PitMod by vertically mixing adjacent model layers until all instabilities throughout the water column are removed. Vertical convective mixing of two adjacent layers is performed either conservatively using volume-weighted mixing, or non-conservatively by using PHREEQC to mix the layers together;
- The rate of oxygen demand in the water column is constant, and has been set to represent a poorly productive (*i.e.*, oligotrophic) lake system.

PitMod utilizes the following inputs to simulate the evolution of physical and chemical properties in the Ajax pit lake:

- Pit void morphometry data for determining the volume, and planar and pit wall areas vs. depth relationships used in the mass and energy balance equations for the pit lake.
- A water balance specifying values for all included inflows and outflows to and from the pit lake (*e.g.*, precipitation, evaporation, and groundwater).
- Concentrations of all included geochemical species and gases in each inflow together with values of pH.
- Time-series of meteorological variables required for the calculation of surface layer heat and mass balances, including:
    - Air temperature;
    - Relative humidity;
    - Evaporation;
    - Precipitation;
    - Incident solar short-wave radiation;
    - Incident solar long-wave radiation; and
    - Surface wind speed.

3. Model Inputs and Assumptions

3. Model Inputs and Assumptions

3.1 Summary of Information and Data Sources

Water quality modelling in pit lakes is based on a conceptual design which incorporates several interrelated layers consisting of hydrologic, geochemical, geologic, and limnologic processes, as described above. The following sections describe each of the input parameters and assumptions used in the Ajax pit lake model.

Input data to the pit lake model were derived from several sources consisting of field observations, environmental baseline studies, web-based climate archives, and site wide water balance and water quality models.

Table 3-1 lists the modelling parameters and the source of the input values. Following this section are detailed descriptions of the methods and assumptions employed in the production of the modelling inputs.

Table 3-1:
Model Input Summary and Data Sources

Process	Parameter	Units	Agency/Company
Climate	Precipitation	mm	KP
	Evaporation	mm	KP/BGC
	Temperature	°C	KP
	Shortwave Radiation	W/m^2	KP/Lorax
	Longwave Radiation	W/m^2	Lorax
	Wind Speed	m/s	KP
	Relative Humidity	%	KP
Pit Morphometry	Elevation Contours	masl	KAM
Water Balance	Pit wall Runoff	m^3/month	BGC
	Disturbed Runoff	m^3/month	BGC
	Lake Surface	m^3/month	BGC
	Natural Runoff	m^3/month	BGC
	Groundwater	m^3/month	BGC
	South MRSF	m^3/month	BGC
	Pond Seepage	m^3/month	BGC
	TSF	m^3/month	BGC
Geochemical Source Terms	Pit wall Runoff	mg/L	Lorax
	Disturbed Runoff	mg/L	KP
	Lake	mg/L	KP
	Natural Runoff	mg/L	KP
	Groundwater	mg/L	KP
	South MRSF	mg/L	KP
	Pond Seepage	mg/L	KP
	TSF	mg/L	KP

Notes: Lorax = Lorax Environmental Services Ltd.; KP = Knight Piesold Ltd.; BGC = BGC Engineering; KAM = KGHM International; TSF = Tailings Storage Facility; MRSF = Mine Rock Storage Facility.

3.2 Meteorological Inputs

The primary driving mechanisms in pit lake modelling include heat, mass, and momentum exchange at the lake surface. These surface exchanges constitute the main energy required for heating, mixing and stratifying the lake. Meteorological inputs required to compute the heat exchange dynamics and meteoric water balance include precipitation; evaporation; downward shortwave and longwave radiation; relative humidity; and wind speed.

The following sections describe the sources and methods used to generate the meteorological inputs to the pit lake model.

3.2.1 Overview

The main source of climate information for the pit lake model meteorological inputs is the 2014 Climatology Report prepared by Knight Piesold Ltd (KP). The objective of the report was to characterize the meteorological conditions at the Ajax project area by estimating long-term climate values through the use of regression analyses between regional and site specific meteorological stations. Long-term data were obtained from nearby regional stations operated by Environment Canada (EC) and the British Columbia Ministry of Forests, Lands and Natural Resource Operations (FLNRO). The AJAXMET climate station has been monitoring temperature, relative humidity, atmospheric pressure, solar radiation, precipitation and wind speed and direction in the project area since August 2010. AJAXMET temperature, precipitation, shortwave radiation, and relative humidity were correlated with concurrent regional or gridded model data to produce long-term estimates and subsequent monthly means. Given the difficulty in correlating site wind observations with regional winds, mean monthly values were simply estimated from the 5 years of AJAXMET data. Evaporation data were unavailable from either the project area or from regional stations and were estimated on the basis of evaporation equations using the synthetic temperatures produced from the regression analysis. Shortwave and longwave radiation were not analysed in the KP report and consequently required analysis by Lorax Environmental Services Ltd (Lorax) using a combination of AJAXMET data, empirical formulations and General Circulation Model (GCM) data from the National Centres for Environmental Protection (NCEP). As the GCM data is provided in gridded binary format, time-series were generated through bi-linear interpolation of 4 bounding model grid points around the location of interest.

Table 3-2 summarizes the station details for the on-site and regional climate stations used in the analysis.

Table 3-2:
On-Site and Regional Climate Station Details

Station Name	Station Type	Latitude	Longitude	Elevation	Start Year	End Year	Total Years of Record
AJAXMET	On-site	50° 38' 32" N	120° 27' 44" W	950	2010	2014	5
Afton	FLNRO	50° 40' 23" N	120° 28' 55" W	780	1988	2014	27
Kamloops Airport	EC	50° 42' 29" N	120° 27' 00" W	345	1953	2014	62

For consistency with the BGC water balance and KP water quality models, climate inputs to the pit lake model were based on the long term cycling of 12 monthly climate means consisting of precipitation, air temperature, downward shortwave and longwave radiation, relative humidity, wind speed and evaporation (Table 3-3). Data sources and time periods used in the calculation of these means are shown in Table 3-2.

Table 3-3:
Synthetic Climate Normals for PITMOD input

Month	Precipitation	Air Temp	Downward Longwave	Downward Shortwave	Relative Humidity	Wind Speed	Evaporation/ Sublimation
	Mm	°C	W/m2	W/m2	%	m/s	mm
Jan	23.4	-4.5	240	36	84	2.0	7
Feb	14.5	-2.4	245	61	75	2.3	7
Mar	11.9	1.5	248	106	67	2.6	12
Apr	19.2	6.5	256	163	57	2.7	40
May	32.8	11.1	276	205	57	2.3	77
Jun	43.4	14.7	293	220	61	2.4	103
Jul	42.4	18.7	302	231	47	2.3	130
Aug	32	17.8	299	197	48	2.1	114
Sep	35.8	12.9	279	141	55	2.3	71
Oct	15.5	5.6	262	81	70	2.2	28
Nov	28	-0.1	247	41	82	2.5	7
Dec	37	-4.9	237	30	84	2.1	7

NCEP Climate Forecast System Reanalysis (CFSR/CFSV2)

The NCEP CFSR dataset is a global, high resolution, coupled atmosphere-ocean-land surface-sea ice system designed to provide atmospheric, oceanic, and land surface output products. Typical resolutions are 0.3 and 0.5 degrees and extend over a 33 year period

between 1979 and 2011. To augment the CFSR data, additional reanalysis data (2011-2013) were obtained from the NCEP Climate Forecast System Version 2 (CFSV2) data archive. Downloaded data included 6-hourly incident longwave radiation and incident shortwave radiation at the 4 bounding model grid points nearest to the mine site.

Regression Analysis

Regression analysis is a method of characterizing meteorological conditions based on regional or gridded model data by calculating long-term, adjusted proxy climate data at the location of primary interest. For meteorological assessments at mine sites, it is common for site specific observations to be of short duration or data gaps occurring as a result of short interruptions caused by broken or malfunctioning instruments. The criterion for employing nearby data is that over the same period, two meteorological parameters must be homogeneous; that is, they represent the same conditions. A key output of regression analysis is the coefficient of determination (denoted by R^2). Values of R^2 greater than or equal to 0.7 indicate good conditions with sufficient homogeneity for calculating proxy data. Regression analyses were conducted by Lorax to generate long-term synthetic downward shortwave and longwave radiation data.

3.2.2 Precipitation

Precipitation data were obtained from the KP 2014 Climatology report. Monthly means were computed by KP from a long-term synthetically generated precipitation time-series (1953-2014) produced for the mine site through regression analysis between the AJAXMET and Kamloops Airport observations. Due to instrumentation problems in the first 2 years at the AJAXMET station, observed precipitation was only available since December 2012. This resulted in 22 months of concurrent monthly data with Kamloops Airport from which the regression analysis was conducted. Mean annual precipitation was estimated to be 336 mm, which is considerably lower than lake evaporation in the area.

3.2.3 Evaporation/Sublimation

Evaporation and sublimation data were obtained from the KP 2014 Climatology Report and the BGC water balance model. Monthly potential evapotranspiration (PET) was equated to lake evaporation and estimated using the temperature based Thornthwaite equation producing a mean annual evaporation of 585 mm. As described in the KP Climatology report, sublimation is the process whereby moisture from snow and ice bypasses the liquid phase and enters the atmosphere directly. It is estimated to be 28 mm for the winter season and assumed to be distributed evenly between November and December. In accordance with the BGC water balance, monthly evaporation values in the

winter months were replaced with 7 mm sublimation values to produce a total annual evaporative loss of 603 mm.

3.2.4 Temperature

Temperature data were obtained from the KP 2014 Climatology. Monthly normals were computed by KP from the long-term synthetically generated air temperature time-series (1988 – 2014) produced through regression analysis between AJAXMET climate station data and concurrent regional temperature observed at the BC Forest, Lands, and Natural Resource Operations (FLNRO) Afton station.

3.2.5 Downward Shortwave Radiation

A long-term synthetic time-series of incident shortwave radiation was generated by Lorax from downscaled NCEP reanalysis model data. Monthly shortwave radiation means were computed from long-term synthetically generated data produced through regression analysis between daily AJAXMET observed shortwave radiation and concurrent interpolated NCEP reanalysis data. The suitability of NCEP reanalysis data is demonstrated in a sample year long comparison time-series plot shown in Figure 3-1 and from the strong correlation (R2 = .86) in the regression analysis (Figure 3-2). The regression equation in Figure 3-2 was applied to the 34-year NCEP shortwave record to generate a synthetic long-term downward shortwave radiation time-series for the project area between the years 1979 to 2013.

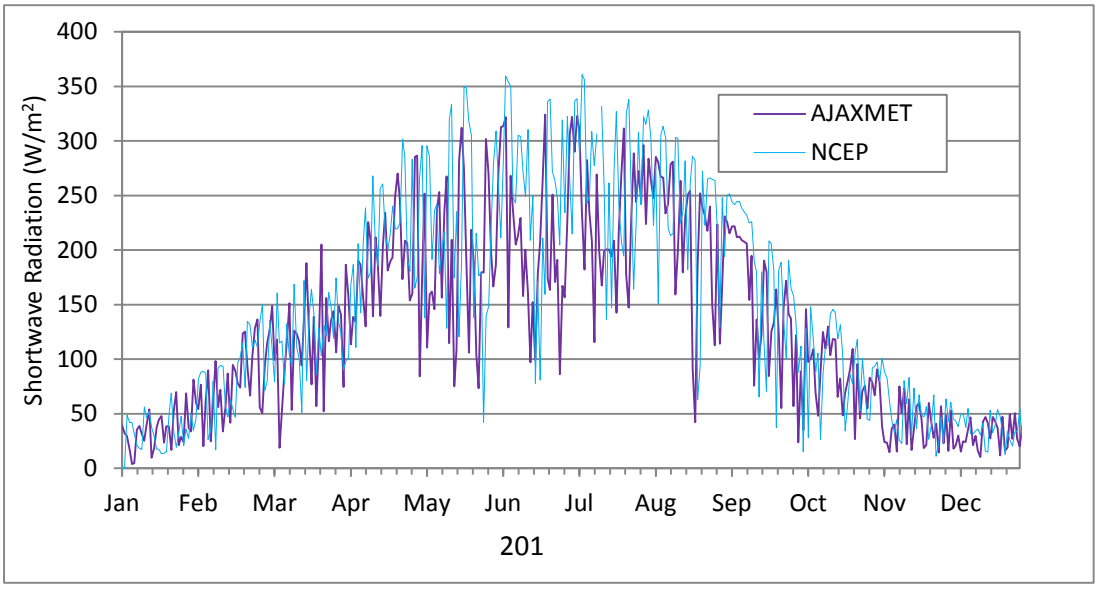

Figure 3-1: Comparison time-series of daily shortwave radiation between NCEP and AJAXMET station (2011)

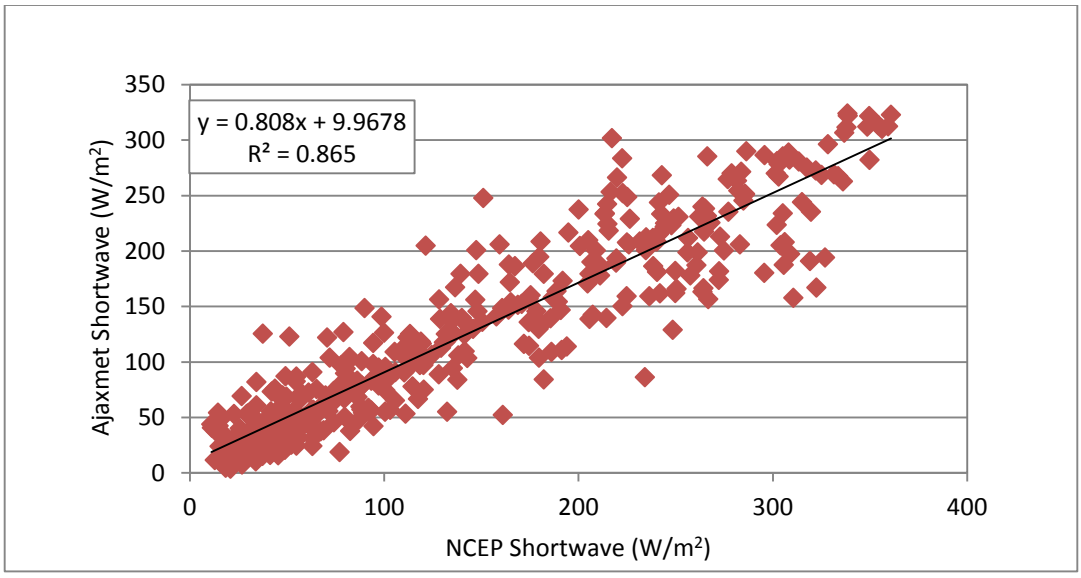

Figure 3-2: Comparison of daily average shortwave radiation between interpolated NCEP model data vs. AJAXMET (2011 – 2012)

3.2.6 Downward Longwave Radiation

A long-term synthetic time-series was generated by Lorax from downscaled NCEP reanalysis model data. Longwave radiation data were not recorded at the AJAXMET weather station or at any of the regional stations and required empirical formulations to estimate daily values. Synthetic daily downward longwave radiation data were produced using regression analysis between calculated short-term longwave based on available observed temperature and relative humidity at the AJAXMET station and concurrent NCEP data. The formulation for estimating longwave radiation using synoptic observations selected for this application was developed by Dilley and O'Brian and is given as follows:

$$L_d = L_{clr} + t_8 c f_8 s\, T_c^4 \quad (1)$$

$$L_{clr} = 59.38 + 113.7(T_a/273.16)^6 + 96.96(w/25)^{1/2} \quad (2)$$

$$t_8 = 1 - e_{8z}(1.4 - 0.4e_{8z}) \quad (3)$$

$$e_{8z} = 0.24 + 2.98\, x10^{-6} e_a^2 exp((3000/T_a) \quad (4)$$

$$f_8 = -0.6732 + 0.6240x10^{-2}T_c - 0.914x10^{-5}T_c^2 \quad (5)$$

Where:

L_d = Incoming incident longwave radiation

L_{clr} = Incoming longwave radiation for clear skies

e_a = Effective atmospheric emissivity

T_a = Near surface air temperature

T_c = Cloud temperature (= T_a – *11°)*

w = Precipitable water

Daily average longwave radiation comparisons between the NCEP model data (1979 – 2013) and calculated longwave radiation (2010 – 2012) for the project area were analyzed over the respective common periods. Acceptable correlation results (Figure 3-3) were achieved with a coefficient of determination value R^2 = 0.72. Using the correlation coefficients derived from the regression analysis with interpolated NCEP records, longwave radiation values at the AJAXMET station were computed for the period 1979 to 2013. Monthly downward longwave radiation means were computed from the long-term synthetically generated records.

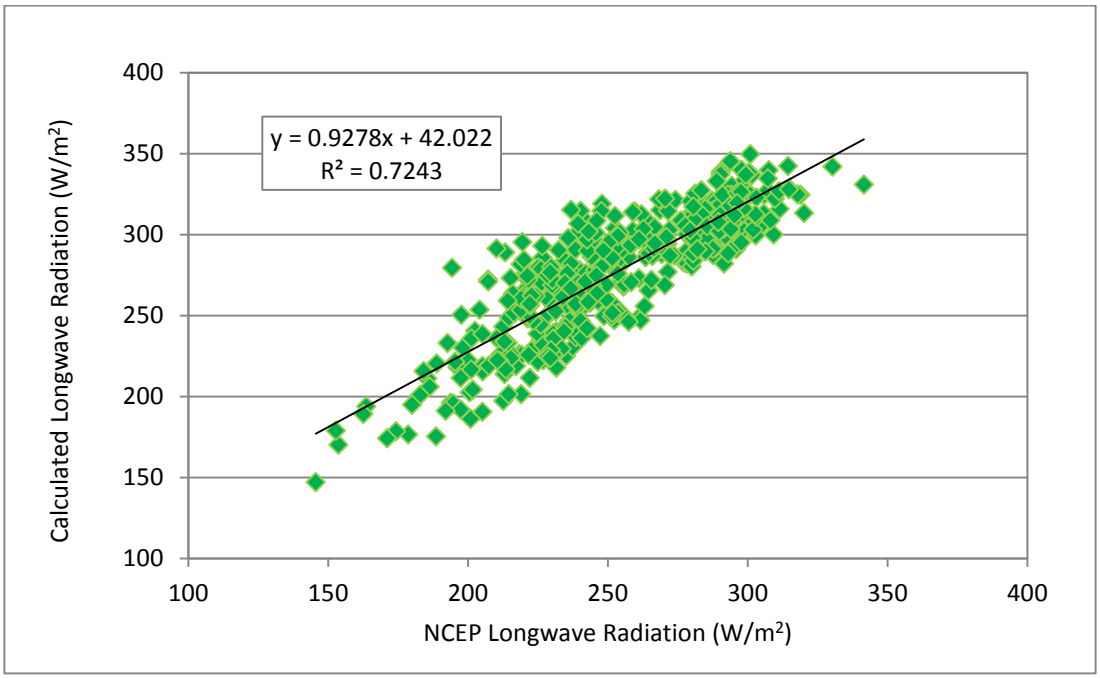

Figure 3-3: Comparison of daily average longwave radiation between interpolated NCEP model data vs. calculated longwave Radiation (2011-2012)

3.2.7 Wind

Wind velocity data were obtained from the the KP 2014 Climatology Report. Monthly means computed by KP directly from the 5 years of AJAXMET wind observations were used for pit lake modelling.

3.2.8 Relative Humidity

Relative humidity data were obtained from the KP 2014 Climatology Report. Monthly normals were computed by KP from the long-term synthetically generated relative

humidity time-series (1988 – 2014) produced through regression analysis between AJAXMET climate station data and concurrent regional relative humidity data observed at the BC FLNRO Afton station.

3.3 Pit Morphometry and Volume

Open pit morphometry was based on the Ajax 2014 ultimate pit (V7B) design (Figure 3-4). Ongoing mine design will slightly change the configuration of the pit but the volumetric proportions are expected to remain similar to those described below. The main physical properties of the pit include a bottom elevation of 435 masl; a maximum highwall elevation of 989 masl; a maximum possible water elevation of 884 masl; and a maximum footprint area of ~239 ha. In-pit backfilling during operations will fill a portion of the western lobe of the pit with ~76.9 Mm^3 of mine rock (Figure 3-5). Backfill extends from the pit bottom at 435 m to a maximum elevation of 925 m; a maximum footprint area of ~66 ha; and a maximum pore water volume of ~20 Mm^3. Excluding pore water volume, the resulting ultimate pit lake that forms will reach a maximum volume of ~333 Mm^3.

Pit lake geometry was incorporated into the pit lake model by defining a matrix of elevations, volumes, and horizontal cross-sectional surface areas between the pit bottom and pit perimeter. Using a contour map of the Life of Mine (LOM) pit area, the volume and surface area of the pit lake were calculated for different lake level elevations. Starting at the bottom of the pit, volume and surface area were calculated at 1 m elevation intervals up to the maximum water level. These data describe the hypsographic (*e.g.* elevation:volume) curves of the pit void and are shown in Figure 3-6 and Figure 3-7 Backfill pore volumes were incorporated into the model as shown by the hypsographic curve shown in Figure 3-8.

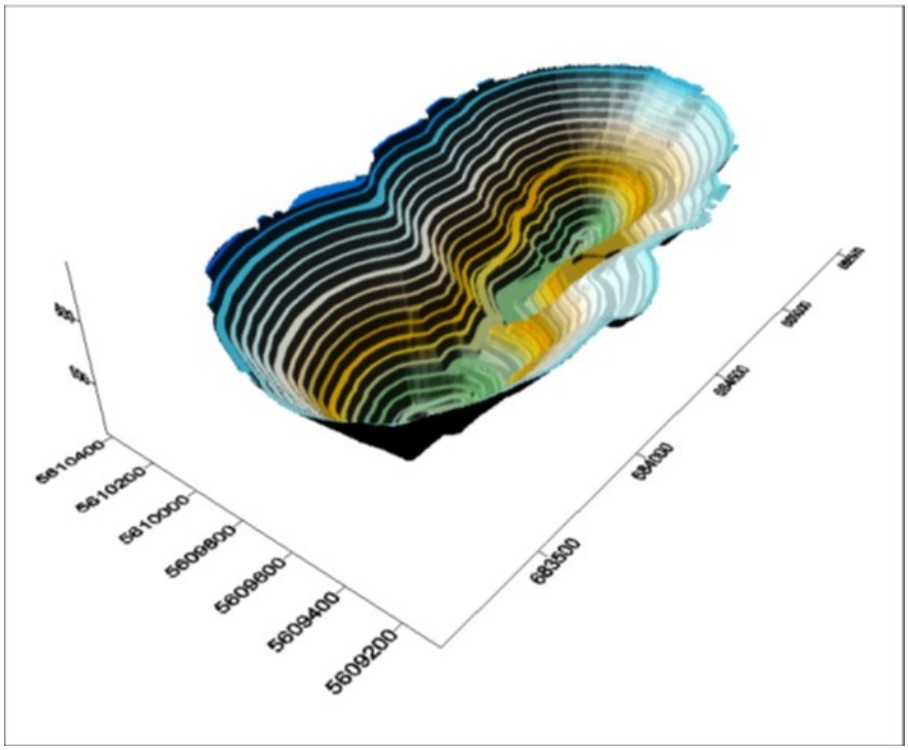

Figure 3-4: Ajax LOM ultimate pit (V7B)

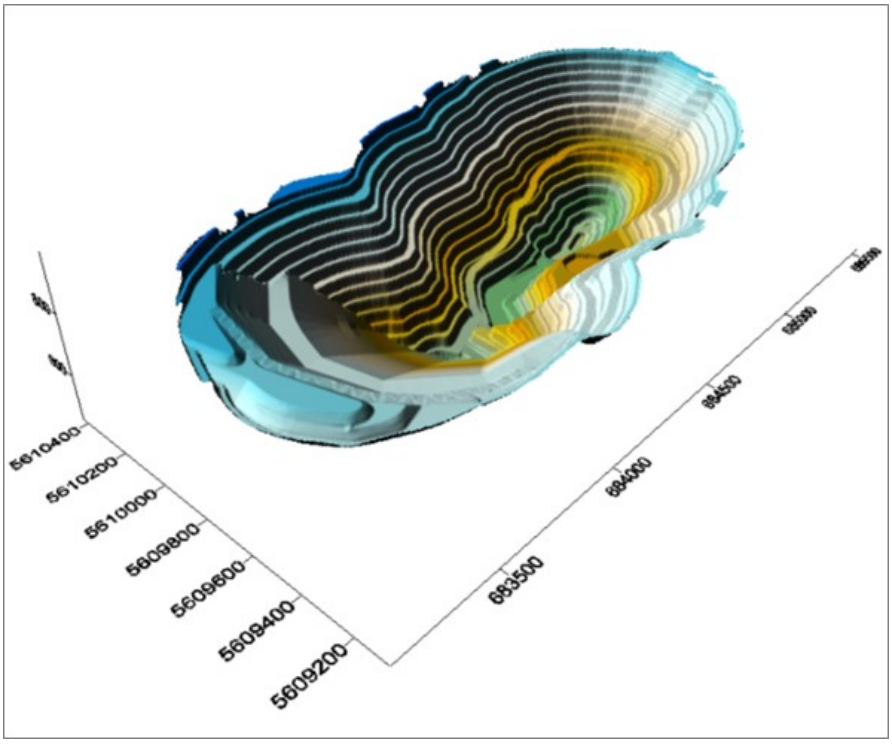

Figure 3-5: Ajax LOM Backfilled ultimate pit (V7B)

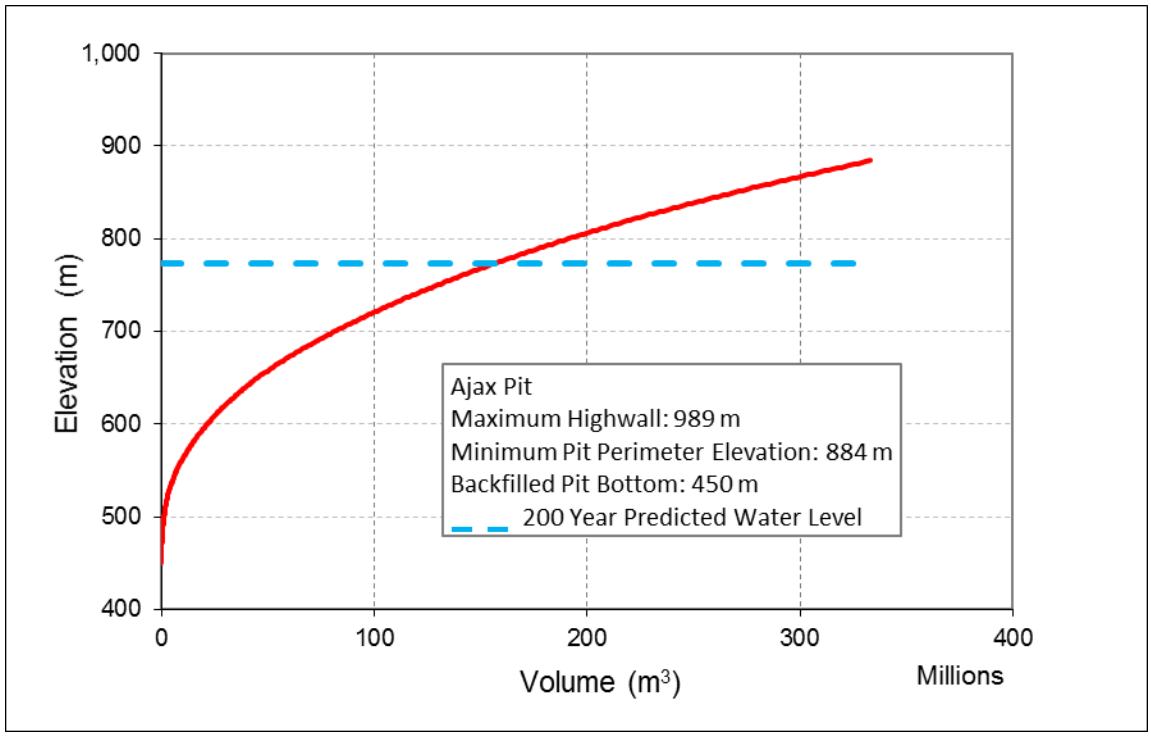

Figure 3-6: Volume-Elevation Curve for Backfilled open Pit

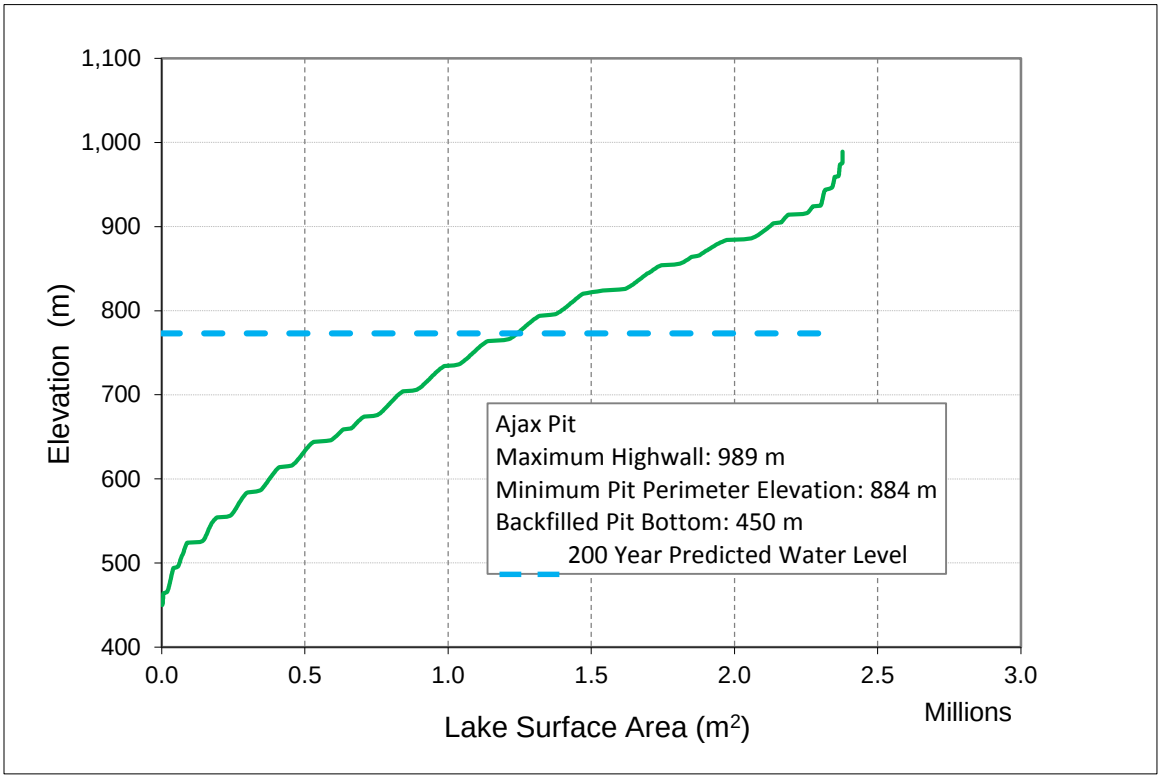

Figure 3-7: Area-Elevation Curve for Backfilled open Pit

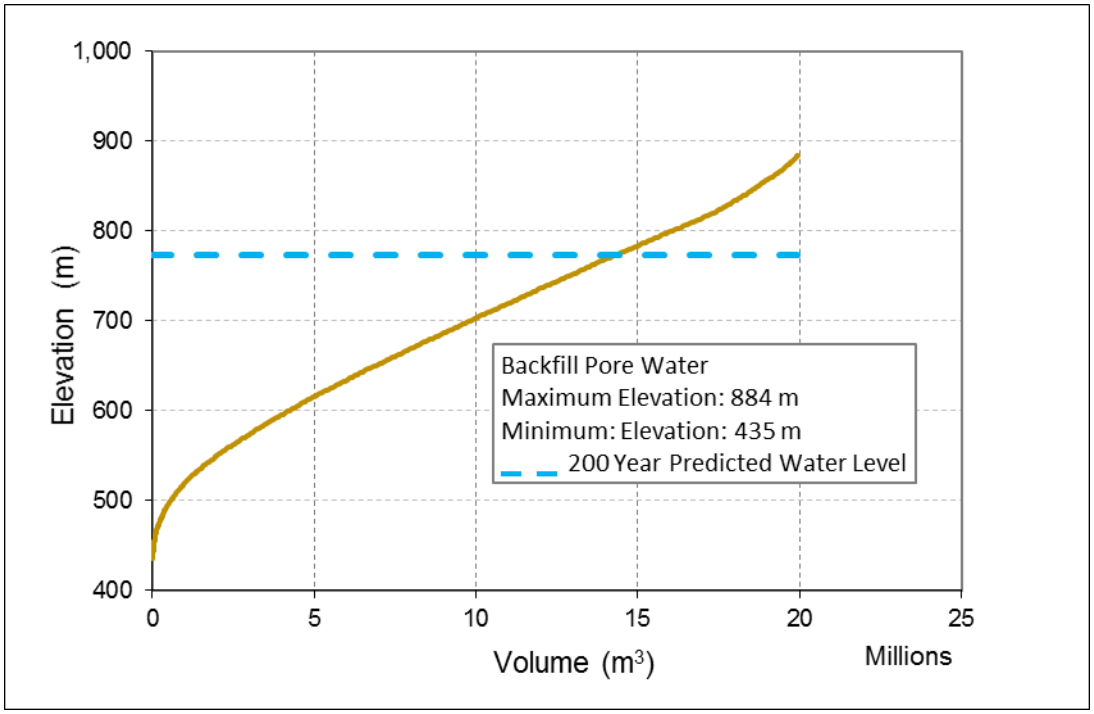

Figure 3-8: Volume-Elevation Curve for Backfilled Pore Space

3.4 Water Balance

A pit lake filling water balance for the Ajax pit was included in the site-wide water balance produced by BGC for the operations and closure mining phases. The water balance was structured in monthly time steps over a 200-year simulation period. As the climate of the Ajax project area is characterized by low total precipitation, high evaporation, and low streamflow rates, post-closure pit lake water levels reached an elevation of 733 m within the maximum simulation period, which is 151 m below the 884 m elevation required to have surface discharge from the pit.

The components of the water balance consist of subsurface groundwater, ten surface inflows, and evaporation (Table 3-4) including disturbed and natural ground surface runoff, lake surface precipitation, South Mine Rock Storage Facility (MRSF) surface runoff, pond seepage, and Tailings Storage Facility (TSF) drainage. All inflow volumes except for *Direct Precipitation to Lake Surface* and *Pit Wall Runoff* were extracted from the water balance provided by BGC. The volume of inflow from precipitation was calculated using the lake surface area and the depth of precipitation for each day. Similarly, pit wall runoff was calculated from the area of pit wall above the lake surface and the depth of precipitation. The total inflow changes somewhat with time as specified in the water balance; however, it remains fairly close to the mean value of 1,552 m^3/day over the course of 200 years.

Table 3-4:
Water Balance inflows and outflows used for the 200-year Ajax PitMod simulation

Source / Sink	Inflow Depth	Water Quality	Volume (10^6 m^3)	Mean density-10^3 (kg m^{-3})
Backfill Runoff	Surface	Time-dependent	1.81	1.216
Groundwater	Distributed over depth of lake[1]	Depth and time-dependent	18.75	-0.535
Groundwater HW	Surface	Time-dependent	6.19	-0.157
Direct Precipitation to Lake Surface	Surface	Fixed	35.08	-0.674
Pit Wall Runoff	Surface	Time-dependent	33.90	-0.032
TSF + South MRSF	Surface	Time-dependent	0.280	1.013
TSF Seepage	Surface	Time-dependent	80.88	1.123
TSF Pond	Surface	Time-dependent	16.28[2]	1.724
Undisturbed Ground	Surface	Time-dependent	4.12	-0.437
Upgradient Pond Seepage	Surface	Time-dependent	3.06	3.254
Jacko Lake Seepage	Surface	Time-dependent	9.32	-.254
Evaporation	Surface	—	-85.97	—

[1] Inflow per unit area of submerged pit wall surface is uniform throughout the depth of the lake
[2] Occurs during the first 4.5 years of filling

The long-term water balance for the Ajax pit lake consists of two distinct phases. During the first 5 years of the closure phase, large volumes of high TDS water from the TSF Pond are discharged into the open pit. The greatest rate of TSF Pond discharge occurs during the first three months of the simulation. The second phase starts after the cessation of TSF inflow, and the geochemical properties of the lake change markedly as the lake adjusts to a new inflow regime.

It is an important feature of the water balance that all of the inflows occur at the surface of the pit lake except for a portion of the groundwater inflows. Groundwater is predicted to discharge to the Ajax pit from both above and below the lake surface. The vertical distribution of groundwater inflows into the pit lake model was apportioned according to a post-processing analysis of tabulated results from the Ajax numerical groundwater flow model developed by BGC. A depth dependent flow distributions from three pit lake water levels (500m, 600m, and 700m) were considered in the post-process analysis (Table 3-5). PitMod applies groundwater flows predicted to discharge into the pit above the lake surface to the upper layer of the model. Each of the groundwater inflows contributes when the pit lake level is located above the lower value in the associated elevation range. The groundwater volume flux within each elevation range below the lake surface is distributed

in proportion to the pit wall area with each model layer. In other words, the groundwater inflow per unit area of pit wall is uniform within each of the four elevation zones.

Table 3-5:
Groundwater Model Depth-Integrated Flows

Average Pit Elevation (m asl)		Average Flows at 500m WL (m^3/day)		Average Flows at 600m WL (m^3/day)		Average Flows at 700m WL (m^3/day)	
From	**To**	**Pit Wall**	**Submerged**	**Pit Wall**	**Submerged**	**Pit Wall**	**Submerged**
931	928	0	0	0	0	0	0
928	926	0	0	0	0	0	0
926	924	0	0	0	0	0	0
924	921	1103	0	1081	0	1116	0
921	906	147	0	142	0	145	0
906	890	48	0	77	0	48.4	0
890	858	10	0	14	0	12	0
858	793	1	0	2	0	4.1	0
793	716	0	0	0.5	0	26.2	10
716	638	0.2	0	2.6	2	5.5	75
638	559	22.3	9	28.7	99	0	40
559	450	73.1	221	0	152	0	81
TOTAL (m^3/day)		**1,405**	**230**	**1,348**	**253**	**1,357**	**205**

3.5 Heat Balance

The heat budget for the lake includes heat energy associated with the temperature of each inflow; surface exchanges of heat with the atmosphere due to evaporation and conduction; and heat added or lost due to incoming or outgoing radiation. The temperature of all surface inflows was set to the mean daily ambient air temperature with an imposed minimum of 0° C. Elevation-dependent groundwater inflow temperatures were incorporated into the model. An analysis of vibrating well piezometer (VWP) temperature data collected over the period 2010 to 2014 revealed a linear relationship between elevation and temperature (Figure 3-63-9) for stations situated near or inside the pit footprint area. Groundwater temperature as a function of elevation (Z) is calculated according to the best-fit linear equation:

$$T_{GW} = -0.0281 * Z + 32.649$$

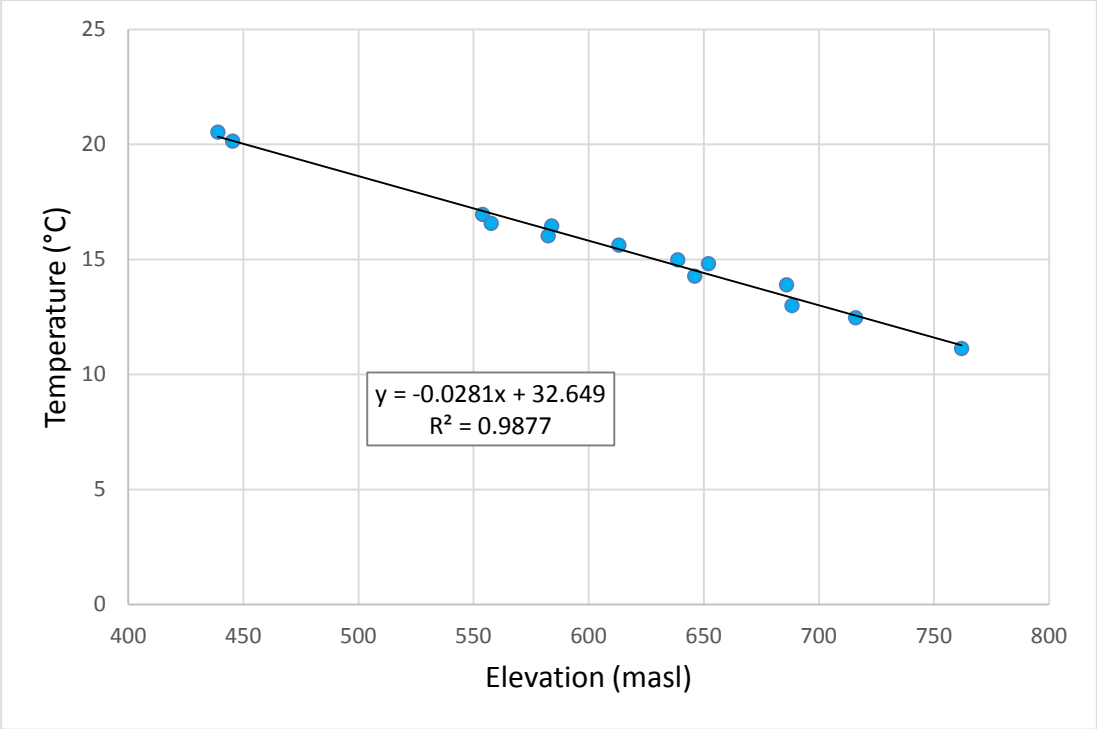

Figure 3-9: Groundwater Temperature-Elevation Curve for open Pit

3.6 Mass Balance

The vertical structure and stability of the Ajax pit lake will be determined by the mixing of groundwater and surface inflows with ambient lake water as determined by their component densities, as well as evaporation and ice formation. The density of each inflow is calculated by first determining the TDS, or salinity, by adding the masses of all dissolved solids in a unit volume of inflow. The resulting salinity and the inflow temperature are then used to calculate density from an empirical equation of state. Densities of surface inflows vary with time through seasonal changes in temperature and/or changes in TDS. Density statistics for each inflow are presented in Table 3-6.

The large volume of relatively dense inflow from the TSF Pond during the first five years establishes a stratified density structure in the pit lake that persists for the remainder of the simulation. Of the surface inflows, only the Upgradient Pond Seepage has a mean density exceeding that of the TSF Pond water comprising the hypolimnion, and this source contributes less than 3% to the total volume inflow (Table 3-6). Therefore, the lake remains stably stratified throughout the 200-year simulation. The relatively low inflow of sub-surface groundwater (16% of the total) mixes with the hypolimnion water, slowly decreasing its density and weakening the stratification over time.

Table 3-6:
Density of Inflows to Pit Lake (σ_t units)

Source	Min	Max	Mean	Median
Groundwater	-1.060	-0.450	-0.535	-0.484
Groundwater (high wall)	-0.992	0.047	-0.157	-0.119
Backfill runoff	0.312	1.810	1.216	1.328
Jacko Lake Seepage	-1.289	0.147	-0.254	0.042
Pit Wall Runoff	-0.485	0.463	-0.032	0.000
Upgradient Pond Seepage	1.565	4.658	3.254	3.585
Precipitation	-1.498	-0.044	-0.674	-0.591
TSF + South MRSF	0.085	1.665	1.013	1.162
TSF Seepage	-1.246	2.957	1.123	1.432
TSF Pond	-1.311	9.150	1.724	0.169
Undisturbed Ground	-1.348	0.137	-0.437	-0.308

3.7 Geochemical Mass Balance

The geochemical mass balance includes all sources of water and solutes that flow into the lake as well as the removal of lake water through evaporation. The mass balance for the Ajax pit lake determines its physical and geochemical properties post-closure. The sources of geochemical loading to the Ajax pit are presented schematically in Figure 3-10 and brief descriptions are provided in Table 3-7.

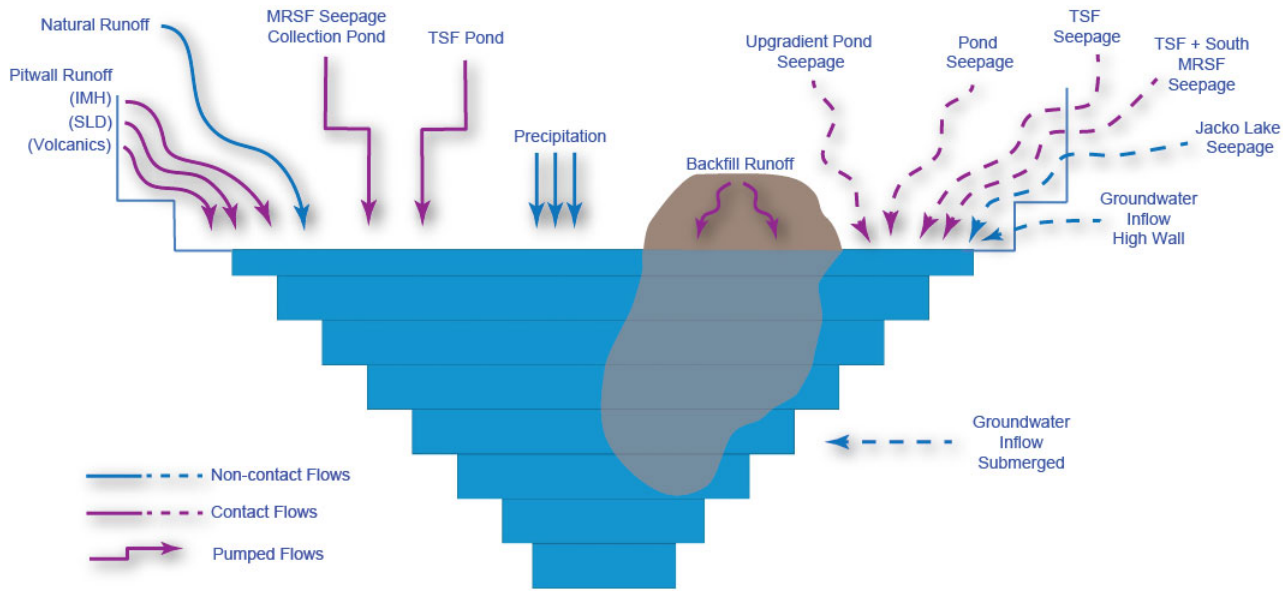

Figure 3-10: Conceptual Loading Model – Ajax Pit

Table 3-7:
Input Terms to Pit Lake Model

Term	Description
Pit Wall Runoff (IMH)	Surface runoff from precipitation falling on pit walls where a portion of the rock units exposed are defined as Iron Mask Hybrid (IMH)
Pit Wall Runoff (SLD)	Surface runoff from precipitation falling on pit walls where a portion of the rock units exposed are defined as Sugarloaf diorite (SLD)
Pit Wall Runoff (Volcanics)	Surface runoff from precipitation falling on pit walls where a portion of the rock units exposed are defined as picrite and mafic volcanics.
Direct Precipitation to Lake Surface	Direct precipitation falling onto the surface of the pit lake
Natural Runoff	Surface runoff from undisturbed catchments
Groundwater	Groundwater flux into the pit below the lake surface
Groundwater HW	Groundwater flux into the pit at the lake surface
MRSF seepage collection pond	Pumped flows from south Mine Rock Storage Facility (MRSF) seepage collection pond.
Pond Seepage	Seepage from the Central Pond
TSF Seepage	Surface runoff from the Tailings Storage Facility (TSF)
Backfill Runoff	Runoff from the mine rock backfill placed in the western pit
Jacko Lake Seepage	Jacko Lake water seeping to the open pit
TSF + South MRSF	Seepage water infiltrating through the mine rock storage facilities
TSF Pond	Tailings pond water that is pumped from the TSF to the pit during the closure phase
Upgradient Pond Seepage	Seepage from pond located north of the open pit

With the exception of pit wall runoff, the water quality terms for each of the pit lake model inflows were output from the closure water quality model prepared by Knight Piesold (Section 3.7.1). Pit wall runoff source terms were generated by Lorax (Section 3.7.2) for each of the three major geologic units (Iron Mask Hybrid (IMH), Sugarloaf Diorite (SLD), and Mafic Volcanics (MAFV) that will be exposed on the ultimate pit wall surface.

3.7.1 Groundwater and Surface Water Inflows from Outside the Pit

Geochemical species that are included for each input into the Ajax pit lake model are listed in Table 3-8 including eight key chemical parameters that are discussed in the report and twenty seven additional ions. Non-detection of mercury (Hg) in laboratory kinetic test leachates prevent the accurate prediction for the individual source concentrations. Similarly, site monitoring data from existing lakes near the Ajax project site confirm that that Hg is not released from Ajax mine waste into the pH-neutral Ajax mine drainage.

Table 3-8:
Chemical species included in the PitMod model of the Ajax pit lake

Key Parameters	Al	As	Cu	Mo
	Na	Se	SO_4	Fe
Other Species	Cl	F	Br	
	Sb	Ba	B	Cd
	Ca	Cr	Co	Pb
	Li	Mg	Mn	Ni
	K	Si	Sr	Tl
	Sn	U	V	Zn
	NH_3	NO_3		

All mass fluxes are discharged at the lake surface with the exception of groundwater inflows that are introduced into the pit lake model both at and below the lake surface, consistent with the groundwater inflow distribution discussed in Section 3.4. The water quality of the groundwater from each source varies on a monthly basis but is identical for all groundwater sources at any particular time. Mean monthly concentrations for each of the surface and groundwater inflows that were determined by the closure water quality model were used as input to the pit lake model. The water quality model report provides details on the temporal variation of monthly pit inflow water quality. The range of water quality for each pit lake inflow is presented in Appendix A. The dissolved oxygen concentration of surface inflows was set to the appropriate saturation value for the inflow water temperature. The dissolved oxygen concentration of groundwater was held fixed at 1 mg/L.

3.7.2 Pit Wall Source Terms

3.7.2.1 Pit Wall Runoff

Geochemical source terms for pit wall runoff of an exposed pit wall are derived by upscaling the geochemical loading rates produced by humidity cells (mg/kg/wk) to the inferred mass of reactive waste rock material for each of the three major mine rock lithologies as well as ore exposed in the pit walls. The exposed rock in the pit walls can be described as a combination of rubble that has accumulated on the benches as well as fractured material in the intact wall. Scaling factors are then implemented to adjust for the hydrogeological and geochemical processes that differ between laboratory kinetic experiments versus the full scale mine-site. For the Ajax pit wall material, the following assumptions were made.

- The final pit walls are expected to be fractured as a result of blasting. Fracturing of the pit walls exposes a greater proportion of the wall rock to weathering and hence wall rock drainage will have the geochemical signature of the respective rock type. The blast damaged zone comprises a crushed zone, fractured zone and an

influenced zone. The crushed zone would be removed for processing or waste dump disposal, and the fractured and influenced zones would remain in place upon closure of the mine and be subjected to ongoing weathering. The penetration depth of the blast influenced zone into the wall rock is dependent on a variety of parameters. Hustrulid (1999) estimated ranges of 0.85 to 1.05 m and 2.65 to 3.15 m for the blast-damaged and the blast-fractured zones, respectively. These estimates are based on controlled blasting and an intermediate rock strength. For the Ajax pit walls, penetration depths of 0.9 and 2.9 m intermediate values from the reported range were chosen for the blast-damaged and the blast-fractured zones, respectively.

- To provide source terms readily adjustable to changing exposures of the pit wall and/or changes in the water balance, it was found appropriate to provide loads per square meter (plan) of exposed unit. Knowing the average slope angle of the pit wall from the bottom to the top of the pit, the approximate length of the according angled surface can be calculated. For the Ajax pit, an average pit wall angle of 45º would yield a tilted exposure factor of 1.41 per m^2 (plan). Multiplying this factor by the thickness of the blast-damaged and blast-fractured zones as well as the bulk density of the material then provides the total mass of rock exposed per m^2 (plan).
- A lab-to-field adjustment for grain size needs to be applied to the wall rock in order to account for the difference in specific surface area between the humidity cell samples and the fractured pit wall rock. It is assumed that 10% of the blast-damaged and 5% of the blast-fractured highwall materials have a grain size distribution comparable to humidity cell samples.
- The incipient hydrogeological regime associated with pit walls differs markedly from waste piles and can be described as primarily fracture-controlled. For the Ajax pit walls it was assumed that 75% of the blast damaged rock will be rinsed by meteoric water on a regular basis and release a geochemical load to the surrounding environment. Providing less exposure in the in-place wall, the contact water factor for the blast-fractured zone was set to 50%. These scaling factors therefore account for the amount of estimated contact water.

The scaled loading rates are subsequently multiplied by the number of weeks within a year and divided by the water volume expected to come in contact with the exposed pit walls per year. The following equation summarizes the above approach used for the derivation of pit wall runoff source terms:

Predicted Runoff Concentrations (mg/L) =

[HC Loading Rate (mg/kg/wk) x 52 wk x Exposed Mass (kg) x Scaling Factors (%)]/ (Annual Runoff Volume)

Certain species (*e.g.*, Al and Fe) are strongly solubility controlled under neutral pH-conditions leading to unrealistically high predicted concentrations even after the application of scaling factors. Therefore, as a last step of drainage quality prediction modelling, the calculated solutions are computed using a thermodynamic speciation model (PHREEQC) in order to further reduce predicted concentration for parameters that are known to be limited by secondary minerals commonly seen in oxidizing mine waste environments. Such minerals include ferrihydrite, gibbsite, silica and gypsum.

To facilitate the input of pit wall loading into the pit lake model, the solubility-limited concentrations are subsequently re-converted into loading rates ($mg/m^2/year$) by multiplication with the annual contact water volume. Table 3-9 provides an overview of the source term loads for neutral and acidic pit wall runoff. Note that the IMH rock does not have acid generating potential such that only a neutral source term is provided for this unit.

Table 3-9:
Predicted Runoff Loads for Mine Rock Units exposed in the Ajax Pit
(mg/m^2/year)

	IMH	SLD (neutral)	SLD (acidic)	MAFV/PICR (neutral)	MAFV/PICR (acidic)	Ore (neutral)	Ore (acidic)
pH	8.0	8.0	6.2	8.0	5.7	8.0	6.1
SO_4	1488	1514	1935	1569	2139	1517	2115
Cl	0.84	1.1	1.0	0.81	0.76	0.98	0.92
F	0.39	0.25	0.24	0.47	0.64	0.27	0.25
Br	1.0	1.0	1.2	1.0	0.99	1.0	1.3
Al	0.0030	0.0031	0.0074	0.0032	0.30	0.0032	0.022
Sb	0.0065	0.0030	0.0028	0.012	0.011	0.0027	0.0025
As	0.039	0.015	0.00060	0.081	0.00060	0.016	0.00060
Ba	0.032	0.029	0.021	0.029	0.021	0.027	0.011
B	0.20	0.16	0.14	0.41	0.34	0.21	0.18
Cd	0.000020	0.00012	0.0013	0.00010	0.0010	0.00034	0.0037
Ca	540	558	490	583	536	574	637
Cr	0.0021	0.0019	0.0017	0.0052	0.0049	0.00049	0.00046
Co	0.00051	0.00067	0.49	0.0016	1.1	0.00065	0.48
Cu	0.011	0.011	2.9	0.011	5.4	0.011	7.5
Fe	0.00029	0.00028	0.0088	0.00028	0.0079	0.00027	0.0063
Pb	0.00023	0.000080	0.00044	0.00014	0.00075	0.000090	0.00049
Li	0.034	0.020	0.050	0.027	0.067	0.018	0.045
Mg	58	54	177	53	180	46	118
Mn	0.021	0.017	0.15	0.027	0.24	0.024	0.21
Mo	0.038	0.66	0.015	1.5	0.030	2.1	0.030
Ni	0.0029	0.0060	1.0	0.12	1.0	0.0018	0.32
P	0.037	0.036	0.011	0.032	0.010	0.040	0.013
K	49	52	32	56	101	53	83
Se	0.0042	0.030	0.079	0.032	0.080	0.080	0.080
Si	6.6	6.6	6.5	6.6	6.5	6.6	6.5
Na	10	11	13	9.0	11	9.3	11
Sr	3.6	3.4	1.7	2.7	1.4	3.4	1.7
Tl	0.000080	0.00016	0.00019	0.00025	0.00090	0.00021	0.00026
Sn	0.00025	0.00025	0.00043	0.00025	0.00016	0.00025	0.11
U	0.0014	0.0052	0.00044	0.00097	0.000080	0.0024	0.00020
V	0.11	0.11	0.0082	0.062	0.0024	0.087	0.0035
Zn	0.013	0.0080	0.060	0.013	0.097	0.0049	0.036

Notes: all loading rates are given in mg/m^2 (plan)/year

3.7.2.2 Release of Stored Loads

Pyrite oxidation occurs at relatively low moisture contents (down to <1%) and may therefore proceed in the unfrozen portions of the pit walls that are not regularly flushed (*e.g.*, Kempton and Atkins, 2000). The formation of the Ajax pit lake after closure will lead to lower portions of the pit wall to be completely flushed. Conceptually, as the pit lake rises, rock surfaces that are not regularly rinsed during sub-aerial exposure will be flushed upon flooding and reaction products that have accumulated during weathering of these exposures will be released and contribute a geochemical load to the aqueous geochemical system. The longer a pit wall is exposed under atmospheric conditions, the larger the stored geochemical load will be as moisture and air will continue to oxidize sulphide minerals. As described in the previous section, a water contact scaling factor was applied for the pit wall runoff geochemistry predictions to account for a limited portion of regularly flushed runoff contact zones as a result of low precipitation rates and occlusion of hydrogeological pathways. Assuming that moisture penetrates all reactive material surfaces, the inverse portion of this scaling factor would hence accumulate the mentioned stored loads. Both grain size and temperature correction factors are applied in the same manner as for the runoff loading model (Section 3.7.2.1). Table 3-10 lists the predicted stored loads accumulating over a year of pit wall exposure for the individual lithological units. These loads are tracked in the pit lake model for the time of pit wall exposure and released as a cumulative mass once inundated.

Table 3-10:
Predicted Annual Stored Loads for the Mine Rock Units exposed in the Ajax Pit ($mg/m^2/year$)

	IMH	SLD (neutral)	SLD (acidic)	MAFV/PICR (neutral)	MAFV/PICR (acidic)	Ore (neutral)	Ore (acidic)
SO_4	3101	21962	58676	23770	63508	79511	212431
Cl	62	82	77	60	56	72	68
F	29	19	17	50	47	20	19
Br	91	93	87	79	74	100	94
Al	11	2.8	7.3	10	27	2.2	5.6
Sb	0.49	0.22	0.21	0.86	0.80	0.20	0.18
As	2.9	1.1	0.21	24	4.5	1.2	0.23
Ba	105	96	142	78	115	22	32
B	15	12	10	31	25	16	13
Cd	0.0013	0.0090	0.097	0.0072	0.077	0.025	0.27
Ca	17004	22100	12677	14247	8173	43732	25086
Cr	0.15	0.14	0.13	0.39	0.36	0.036	0.034
Co	0.038	0.050	37	0.12	85	0.048	35
Cu	1.2	1.7	521	1.3	397	1.8	555
Fe	0.99	1.0	0.65	0.90	0.58	0.72	0.47
Pb	0.017	0.0060	0.033	0.010	0.056	0.0066	0.036
Li	3.3	1.5	3.7	2.0	5.0	1.4	3.3
Mg	7551	5092	13111	8276	21309	3387	8722
Mn	1.6	1.3	11	2.0	18	1.8	16
Mo	2.8	49	1.1	112	2.5	156	3.5
Ni	0.22	0.45	80	8.7	1558	0.13	24
P	2.7	2.6	0.84	2.4	0.75	3.0	0.93
K	9890	6157	3602	38603	22580	5680	3322
Se	0.43	0.85	2.2	1.1	2.7	1.9	4.9
Si	5330	4876	20151	5447	22510	3933	16253
Na	778	780	955	671	822	687	841
Sr	285	253	127	202	101	251	126
Tl	0.0061	0.012	0.014	0.056	0.067	0.016	0.019
Sn	0.30	0.061	0.032	0.023	0.012	16	8.3
U	0.10	0.38	0.032	0.072	0.0061	0.18	0.015
V	24	15	0.61	4.6	0.18	6.5	0.26
Zn	0.96	0.60	4.4	0.97	7.2	0.36	2.7

Notes: all loading rates are given in mg/m^2 (plan)/year

3.7.2.3 Timing of NP and Sulphur depletion

The time required for the initiation and cessation of loading rates and stored load accumulation is discussed in this section. The pit lake model accounts for three time related changes to loading and accumulation in the open pit including:

- Time for the implementation of NP-depleted loading rates from PAG rock,
- Time for the depletion of S from PAG rock, and
- Time for cessation of stored load accumulation from NPAG rock.

The loading rates from PAG rock exposed on the pit wall unit were switched from neutral to acidic in the pit lake model. Proportions of PAG material and the estimated lag time for NP depletion of each PAG pit wall unit are listed in Table 3-11 below. The proportion of PAG materials that will eventually become NP-deplete is discussed, in some detail, in Lorax (2015). All PAG pit wall from each respective unit is given an acidic loading rate based on the time required to deplete 25th percentile associated with that unit. The time frame required to deplete neutralization potential is related to the initial modified NP as well as the sulphur content of a sample releasing acidity and therefore driving the NP depletion rate. The rationale and approach used in the calculation of NP depletion rates and the onset of net acid release are also provided in Lorax (2015).

Time for the depletion of the non-sulphate sulphur from the PAG rock is calculated based on the acidic sulphide oxidation rates once the NP has been depleted. The PAG S depletion times listed in Table 3-11 are based on the average sulphide content from each of the PAG units exposed on the pit walls. The calculations conservatively assume that sulphide is not depleted from the PAG units prior to NP depletion.

Stored loads from the NPAG rock exposed on the pit walls are assumed to stop accumulating at the time when the S content from the NPAG rock is predicted to be depleted. Calculations conservatively assume that runoff loads are continuously applied throughout the entire duration of the pit lake model simulation.

Table 3-11:
Proportions of PAG mine rock in pit wall exposures and the time to NP depletion, S depletion and cessation of stored load accumulation

	PICR/MAFV	SLD	Ore	IMH
PAG %	14%	23%	26%	-
Time to NP depletion (years)	45	27	32	-
Time for PAG S depletion (years)	134	110	117	-
Time for cessation of NPAG stored load accumulation (years)	91	83	85	43

4. Results and Discussion

KGHM

4. Results and Discussion

4.1 Physical Structure

The evolution of physical properties in the Ajax pit lake is dictated by values of the meteorological inputs, the water balance, the geochemistry and temperature of the inflows, evaporation, and ice formation discussed in the previous sections. The cumulative inflows and outflows for each component of the water balance over 200 years are shown in Figure 4-1. By Year 200 the pit lake has achieved a depth of approximately 290 m and the largest source of water is runoff from the TSF Seepage.

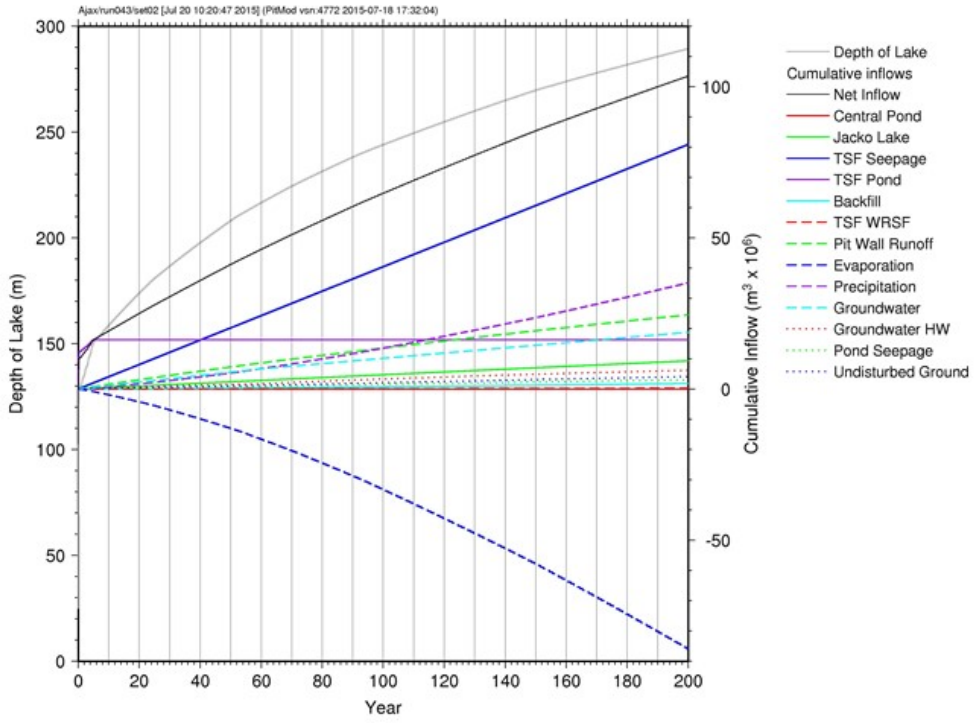

Figure 4-1: Cumulative simulated water balance for all inflows and outflows after 200-years in the Ajax pit lake

Over the 200-year simulation period 35.1 M m^3 of direct precipitation enters the lake surface and 86.0 M m^3 evaporates, for a net loss of 50.9 M m^3 of fresh water from the lake over 200 years. The pit fills because the groundwater, pit wall and other surface inflows add 165.7 M m^3 to the lake over this period for a net volume addition of 114.8 M m^3.

The evolution of physical properties in the Ajax pit lake over the 100-year model simulation is illustrated by the spatial and temporal distributions of temperature, salinity and stability (Figure 4-2). The sum of the mass concentrations of each species yields the

mass concentration of total dissolved solids (salinity) in the lake. Temperature and salinity are then used to calculate water density.

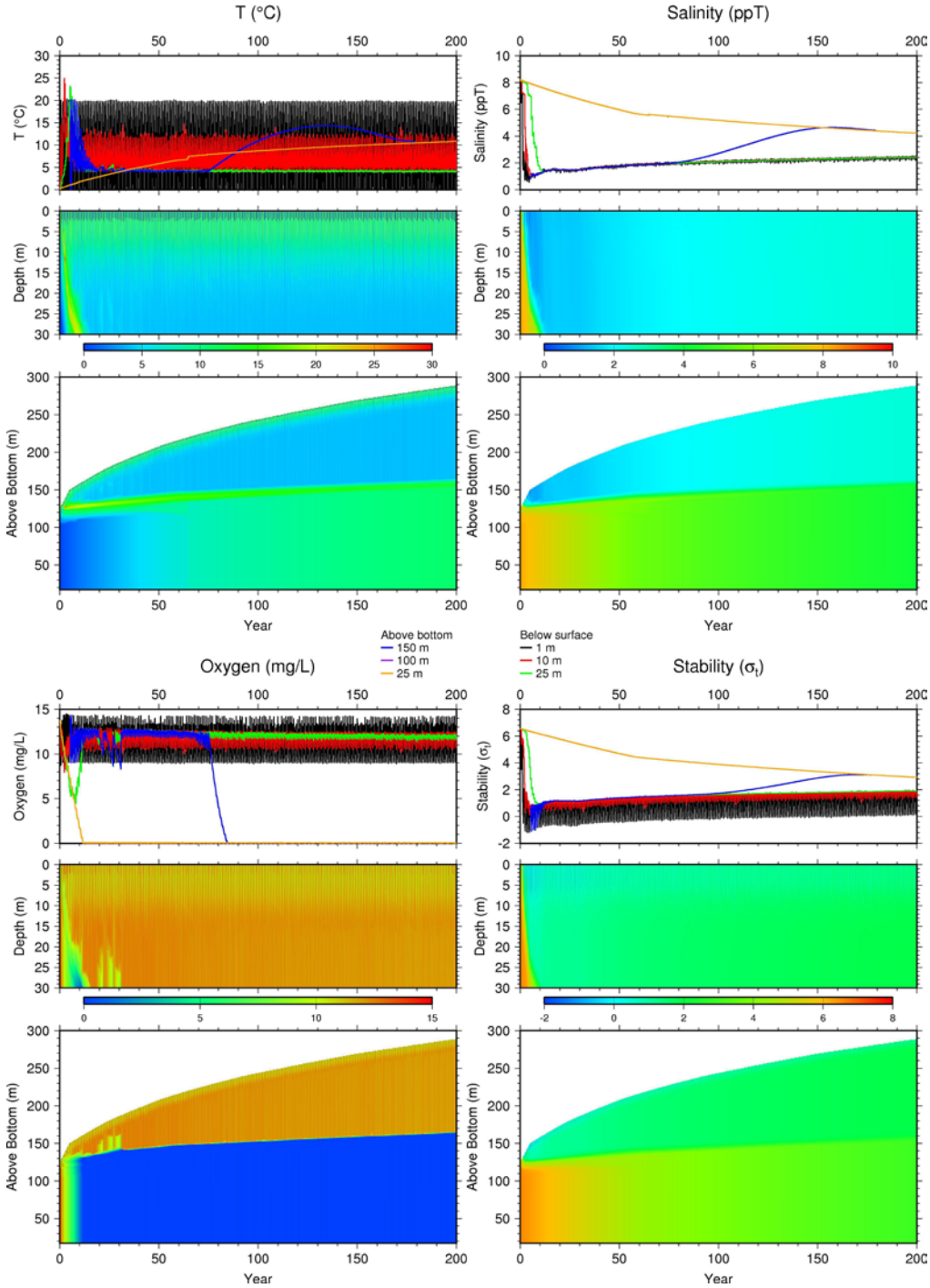

Figure 4-2: Simulated distribution of temperature, salinity, oxygen (DO) and stability. Values are shown for the entire pit lake (bottom); upper 30 m (middle); and depths of 1, 10, and 25 m; and elevations of 25, 100, and 150 m (top). Units of stability are σ_t (density-1000 kg/m^3).

PitMod utilizes a special density term called stability when assessing the vertical stability of a lake. Stability is calculated in the same way as density using temperature and salinity, but without including the effect of water compressibility that occurs below the surface. Both stability and density values are usually expressed as σ_t (density-1000 kg/m^3). Thus, a value for σ_t of 0.5 corresponds to 1000.5 kg/m^3. When PitMod assesses the stability of the water column in a pit lake it compares the density of adjacent layers in the model and removes any instabilities caused by denser water overlying less dense water by instantly mixing the two adjacent layers together.

The water balance for the Ajax pit lake is dominated during the first five years of the model simulation by the TSF Pond inflow, which accounts for 82% of the net inflow during the first five years, and 14.2% of the total net inflow over 200 years. During the first 14 months the density of the TSF Pond discharge ranges from 5 to 9 σ_t, and the combined net inflow has a density during this period of from 2 to 6 σ_t. After this short period of high-density inflow the combined inflow density decreases markedly for the remainder of the simulation. This initial influx of dense water immediately establishes a highly stratified system where the initial volume of dense water is covered by a steadily deepening layer of much less dense water resulting from the combined surface inflows. The depth of the surface layer increases to 130 m after 200 years, while the density difference across the pycnocline decreases steadily over the same period due to mixing with low-density groundwater. The epilimnion and hypolimnion are separated by a strong pycnocline and chemocline.

The temperature plot in Figure 4-2 shows that the modeled pit lake develops a thermocline at a depth of 25-30 m after approximately five years. The water layer above the thermocline remains oxic, while deeper pit lake waters become anoxic by Year 10 following the cessation of TSF Pond inflow after five years. The lake becomes anoxic below 25-35 m depth and remains anoxic throughout the remaining 195 years of the model simulation.

The seasonal variation of temperature, salinity, dissolved oxygen (DO), and stability during years 95 and 96 of the model simulation are more clearly illustrated in Figure 4-3 and Figure 4-4. The upper panel in Figure 4-3 shows time-series at depths of 1, 10 and 25 m below the surface, and at elevations of 25, 100, and 150 m above the bottom. The middle panel shows the upper 30 m of the lake, while the bottom panel shows the entire lake.

The single largest seasonal influence on the pit lake is the variable air temperature that affects ice formation on the surface of the lake and oxygen concentrations. The period of surface ice formation and melting in the model extends from early December through the third week of April. During ice formation pure water is transferred from the surface layer

to the ice sheet, resulting in slight increases of solute concentrations and water density in the surface layer of the model. The water in the model layer directly under the ice is maintained at a temperature of 0° C.

The seasonal variability of temperature, salinity, DO, and stability are also shown in Figure 4-4, which includes 12 monthly profiles taken from Year 95. Profiles from other years during the last half of the simulation are similar. Profiles from mid-December to mid-March are coloured blue; profiles from mid-May to mid-August are coloured red; profiles from mid-September to mid-November are coloured cyan; and the profile at the start of the ice-free period in mid-April is coloured green.

The four variables in Figure 4-4 all exhibit at least some seasonal variability in the upper 20 m – a depth typical for the surface wind-mixed layer within which seasonal variability is most pronounced. The greatest variability in the surface layer is exhibited by temperature, while salinity exhibits the least variability. Below 25 m depth the values of each variable remain nearly constant throughout the year.

Temperature in the modelled pit lake remains nearly constant at 4° in the layer from 30 m to 90 m depth. From 90 to 97 m the temperature increases to a maximum of 15° before decreasing to 8.5° at 102 m, where it remains constant to the bottom at 160 m. The thermal structure of the simulated Ajax pit lake contrasts with a typical natural lake where bottom waters are usually at or near 4°, the temperature of maximum density of fresh water. The portion of the pit lake above 90 m depth behaves like a classic natural lake. Below 90 m depth the thermal structure of the Ajax pit lake reflects the contribution of salinity to density below the pycnocline. Specifically, the decrease in density that would result in a natural lake from an increase in temperature is offset by a larger contribution to the density from the increase in TDS.

Salinity in the pit lake remains nearly constant from the surface to 90 m depth, where it increases from 2.1 to 5.2‰ over the next 10 m. There is some variability evident in the upper 5 m resulting from precipitation, and ice formation and melting. The constant salinity profile from 5 to 90 m depth is indicative of a well-mixed upper layer in the lake. Below 100 m depth the salinity remains constant at 5.2‰. The strong pycnocline between 90 and 100 m and the absence of seasonal variability in water properties indicates that there is little or no intrusion of water from above 90 m depth into the layer below 100 m depth at this point in the model simulation.

DO exhibits variability in the upper 10 m due to the temperature dependence of the saturation concentration of DO; that is, cold water can hold more dissolved oxygen than warm water. Oxygen concentration decreases to zero below 45 m depth and remains zero below 45 m depth throughout the year.

The profile of stability in Figure 4-4 corresponds to variations in density with depth. Density is a function of temperature and salinity and the model requires that stability increase monotonically with depth to avoid instabilities. Since the lake's salinity varies little from the surface to 90 m depth throughout the year the seasonal variations in stability in the upper 20 m are due almost exclusively to seasonal variations in temperature. The water density in the wind-mixed surface layer of the lake varies significantly over the course of a year due to large seasonal fluctuations in the upper layer temperature and, to a much lesser degree, to salinity variations in the upper 5 m. Surface wind provides kinetic energy for upper-layer mixing, while the surface layer temperature of the lake varies in accordance with fluctuations in the modelled inputs for solar energy; air and surface inflow temperatures; heat fluxes associated with precipitation and evaporation; and wind speed. The vertical structure of the Ajax pit lake at this point in the simulation is characterized by a strong pycnocline separating the oxygenated epilimnion from the underlying, anoxic hypoliminion, with the transition occurring between 90 and 100 m depth.

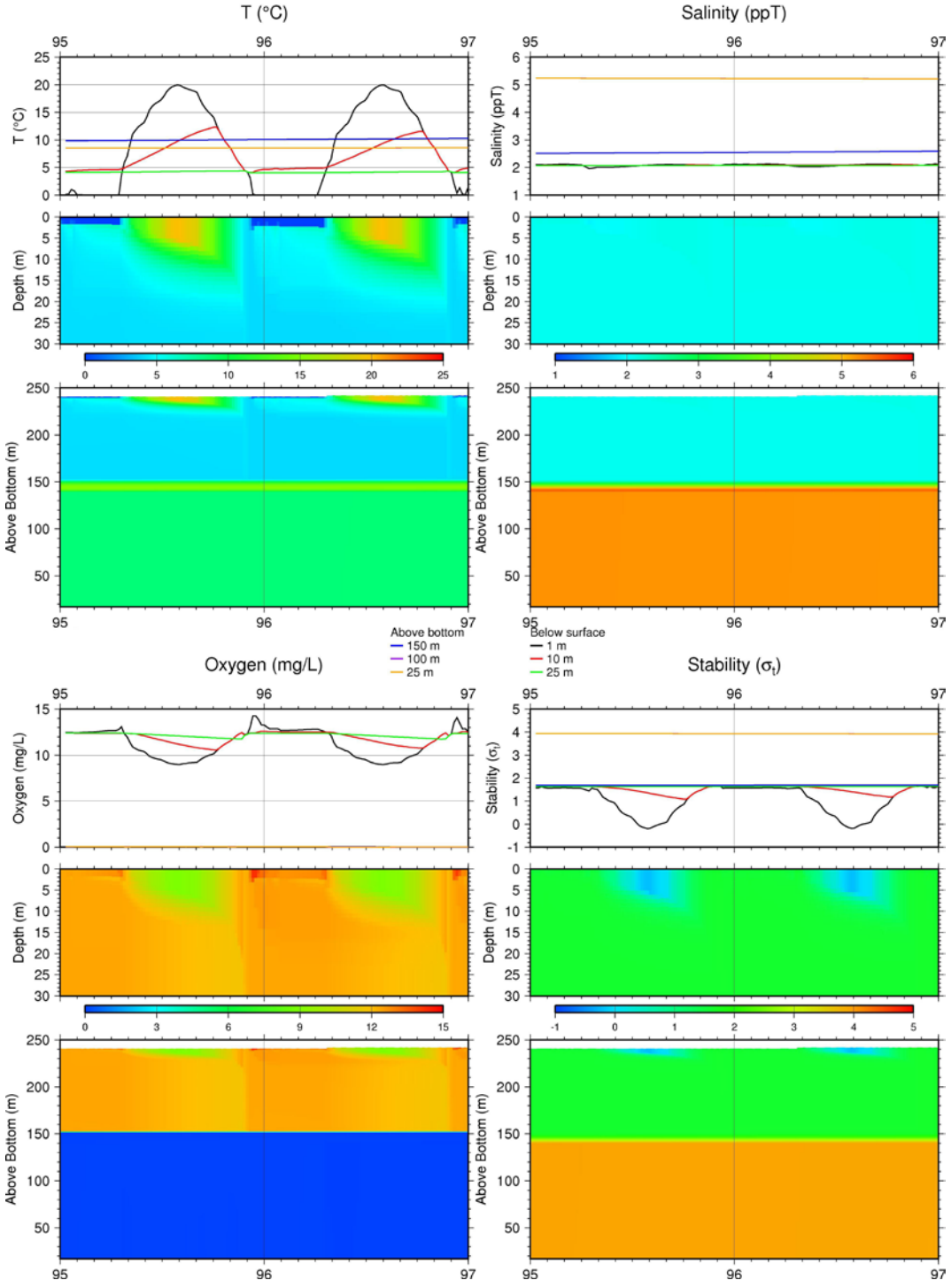

Figure 4-3: Simulated vertical and temporal distribution of temperature, salinity, oxygen (DO), and stability during Years 95 and 96. Values are shown for the entire pit lake (bottom); upper 30 m (middle); and depths of 1, 10, and 25 m; and elevations of 25, 100, and 150 m (top)

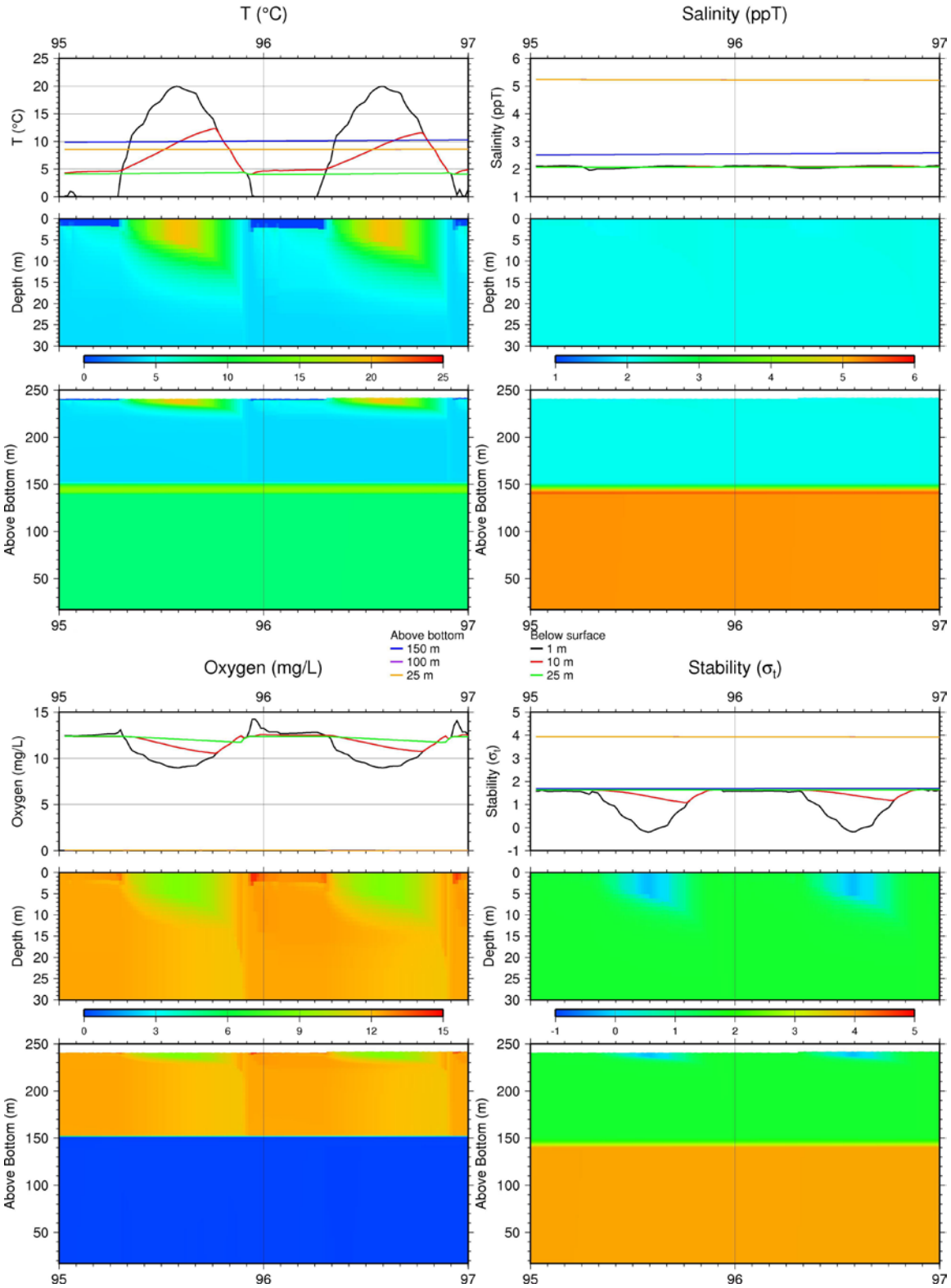

Figure 4-4: Monthly vertical profiles of temperature, salinity (TDS), DO, and stability during Year 95 of the Ajax model simulation

4.2 Water Quality

The Ajax pit lake simulation was run in PitMod's conservative mode, where all interactions between chemical solutes are dealt with by volume-weighted mixing of water masses. Water quality inputs to the pit lake model that were obtained from the site wide water quality model (Section 3.7.1) and pit wall runoff (Section 3.7.2) were developed using conservative assumptions, which compounds the level of conservatism inherent in the predicted pit lake water quality. The Ajax pit lake simulation indicates that two distinct chemical regimes will develop in the lake. An upper oxic layer (epilimnion) will overlie a lower anoxic layer (hypolimnion) separated by a chemocline. During the initial 5 years of filling, 16.3 M m^3 of dense saline TSF Pond water is pumped into the open pit. This water contributes 13% of the total 200-year lake volume and has a major influence on the physical stratification of the lake (Section 4.1) and on the water chemistry in the lower portion of the lake. Although the dense bottom waters are initially oxic, anoxia is predicted to develop for these waters within 6 years and persist for the duration of the model simulation. Conversely, the upper layer remains well mixed and oxic throughout the model simulation.

The temporal and vertical distribution of selected chemical species concentrations over the 200-year Ajax model simulation are presented in Figure 4-5 and Figure 4-6. Monthly vertical profiles of the same species during Year 95 are shown in Figure 4-7 and Figure 4-8.

4.2.1 Hypolimnion

Initially the water chemistry in the lower depths of the lake is equivalent to the TSF Pond chemistry, which evolves over time by mixing with lower TDS groundwater inflows. For most parameters this mixing results in decreasing concentrations over time (Figure 4-5 and Figure 4-6). However, redox sensitive species that have higher concentrations in the groundwater such as iron (Fe) and manganese (Mn), have concentrations that increase in the anoxic bottom waters during the 200 year simulation.

The monthly vertical profiles of the major species concentrations during Year 95 highlight the absence of seasonal variability in water quality below a depth of 100 m, with predicted concentrations at depth remaining virtually constant throughout the year (Figure 4-7 and Figure 4-8). The major ions sodium (Na) and sulphate (SO_4) achieve and maintain their overall maximum concentrations in the lower portion of the lake and have lower values at the surface. Conversely, arsenic (As), copper (Cu), and selenium (Se) have lower concentrations in the lower portion of the lake's water column. Although there is no significant seasonal variation in the hypolimnion water quality the long-term trends due to mixing with groundwater are illustrated in Figure 4-5 and Figure 4-6.

4.2.2 Epilimnion

The pH of the pit lake is predicted to remain circum-neutral to slightly alkaline. Although a small portion of the pit wall (< 10%) is predicted to release acidic runoff in the latter portion of the simulation, the acidic runoff accounts for < 2% the total pit inflows and are offset by alkalinity from NPAG portions of the pit wall and the other surface and seepage flows discharging to the pit lake surface.

Referring to the time-series at depths of 1, 10 and 25 m in the upper panels of Figure 4-5 and Figure 4-6, all species except for Fe achieve a 50-year maximum concentration during the first three months of the Ajax model simulation and then decrease through Year 5, which primarily reflects the initial concentrations of the TSF pond water. Following Year 5, concentrations in the hypolimnion increase, due to the influence of other inputs to the surface of the pit lake once discharges from the TSF Pond dewatering are completed.

The concentration increases during the 200 year model simulation as illustrated on Figures 4-5 and 4-6 are due to a number of factors including:

- net loss of dilute non-contact water from the lake due to evaporation,
- rinsing of stored loads from pit walls as the pit lake surface rises, and
- increasing annual loads from TSF seepage.

The single largest factor producing the increasing concentrations in the upper portions of the pit lake are increased loading rates associated with the TSF seepage, which continue to increase throughout the 200 year simulation. The predicted range of Fe concentrations in the epilimnion is considered an overestimation as the particulate Fe would not be expected to accumulate in the water column but rather be transported to the lower portion of the lake.

Seasonal concentration fluctuations are expected for many parameters in the upper 15 m of the water column due to variable inflow rates and chemistry as illustrated in Figure 4-7 and Figure 4-8. Seasonal concentration fluctuations are observed for Al, As, Cu, Mo and Se. Major ion concentrations including Na, SO_4 and Fe are predicted to be more stable and only minor seasonal concentration fluctuations are expected near the lake surface.

The range of concentrations predicted for the near surface waters are tabulated and compared to BC wildlife guidelines for a subset of water quality parameters in Table 4-1. Application of aquatic life guidelines to the pit lake water quality was not considered an appropriate guideline since the pit lake is a sink for groundwater flow and will not discharge to the adjacent surface water bodies. Migratory birds and bats are wildlife that have the potential to access the pit lake. The model predicts that once the pit lake has been established, Mo and Se will consistently exceed BC Wildlife water quality guidelines. Over time, As is also predicted to increase above the wildlife guidelines. An adaptive management approach would be taken to minimize the potential effect if wildlife are found to use the pit lake.

Table 4-1:
Summary of predicted concentrations near the surface of the pit lake in years 1 to 10; years 11 to 100 and years 101 to 199.

		Year 1 - 10			Year 11 - 100			Year 101 - 199			BC WQG
		Min	Max	Median	Min	Max	Median	Min	Max	Median	
Al	ppm	0.001	0.005	0.002	0.002	0.005	0.004	0.004	0.005	0.005	5
Ammonia	ppm	0.031	0.521	0.325	0.162	0.564	0.211	0.132	0.174	0.148	-
As	ppm	0.003	0.022	0.005	0.006	0.019	0.012	0.019	0.039	0.028	0.025
B	ppm	0.051	0.422	0.073	0.072	0.177	0.113	0.169	0.340	0.249	5
Ba	ppm	0.017	0.054	0.025	0.027	0.070	0.051	0.062	0.085	0.075	-
Br	ppm	0.14	1.18	0.24	0.26	0.57	0.44	0.54	0.81	0.67	-
Ca	ppm	158	641	242	259	493	431	460	529	507	-
Cd	ppm	0.0000	0.0000	0.0000	0.0000	0.0001	0.0001	0.0001	0.0002	0.0002	-
Cl	ppm	18	468	51	53	85	77	75	85	83	-
Co	ppm	0.001	0.003	0.001	0.001	0.004	0.002	0.003	0.006	0.005	-
Cr	ppm	0.001	0.002	0.001	0.001	0.002	0.001	0.002	0.004	0.003	-
Cu	ppm	0.002	0.028	0.004	0.004	0.041	0.014	0.032	0.056	0.045	0.3
F	ppm	0.10	1.39	0.21	0.23	0.46	0.38	0.43	0.59	0.52	1
Fe	ppm	0.068	0.226	0.152	0.214	0.411	0.315	0.372	0.484	0.441	-
K	ppm	8	138	19	20	37	32	34	40	38	-
Li	ppm	0.005	0.032	0.007	0.007	0.016	0.011	0.015	0.029	0.022	-
Mg	ppm	22	257	46	48	85	69	80	113	97	-
Mn	ppm	0.104	0.441	0.255	0.301	0.596	0.448	0.546	0.748	0.663	-
Mo	ppm	0.105	1.006	0.169	0.182	0.464	0.327	0.442	0.779	0.601	0.05
Na	ppm	24	344	54	58	105	86	98	131	116	-
Ni	ppm	0.003	0.025	0.005	0.005	0.016	0.010	0.014	0.022	0.019	-
Nitrate	ppm	0.19	3.87	2.37	0.53	4.17	0.94	0.30	0.58	0.40	100
P	ppm	0.00	0.05	0.02	0.04	0.14	0.11	0.13	0.19	0.16	-
Pb	ppm	0.0001	0.0001	0.0001	0.0001	0.0005	0.0004	0.0004	0.0006	0.0005	0.1
Sb	ppm	0.001	0.019	0.002	0.003	0.006	0.005	0.006	0.010	0.008	-
Se	ppm	0.003	0.009	0.003	0.003	0.010	0.006	0.009	0.020	0.014	0.002
Si	ppm	2	23	5	5	10	8	10	12	11	-
Sr	ppm	0.8	13.3	1.7	1.7	3.3	2.6	3.1	4.7	3.9	-
Sulphate	ppm	302	6764	772	808	1399	1201	1308	1624	1495	-
U	ppm	0.002	0.038	0.005	0.005	0.009	0.007	0.008	0.011	0.010	-
V	ppm	0.005	0.009	0.007	0.008	0.029	0.018	0.028	0.058	0.042	-
Zn	ppm	0.003	0.064	0.007	0.008	0.015	0.012	0.015	0.021	0.018	-

Shaded cells denote predicted exceedance of BC Wildlife water quality guidelines

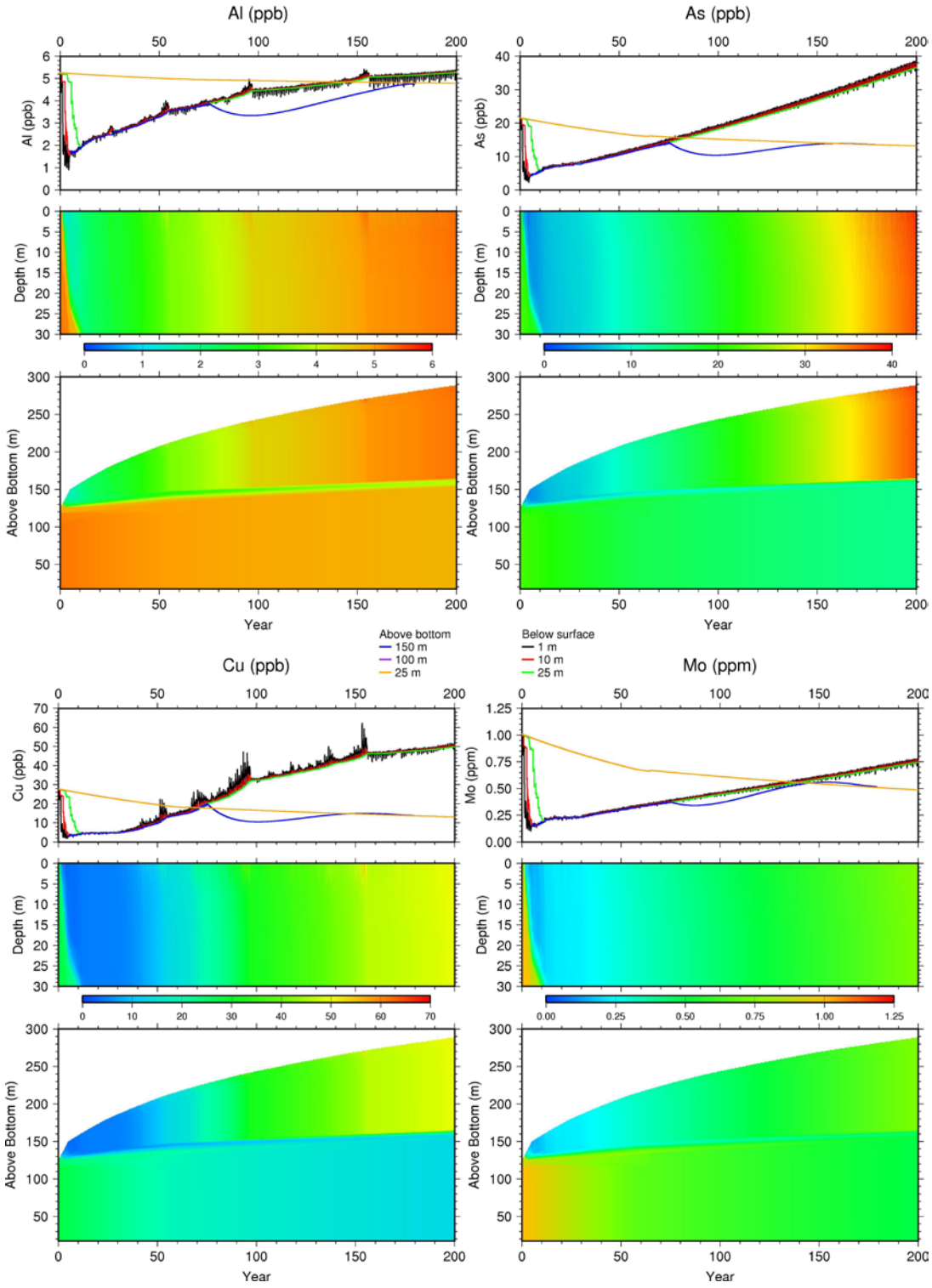

Figure 4-5: Vertical and temporal distribution of Al, As, Cu, and Mo over 100 years from the Ajax pit lake simulation. Values are shown for the entire pit lake (bottom); upper 30 m (middle); and depths of 1, 10, and 25 m; and elevations of 25, 100, and 150 m (top)

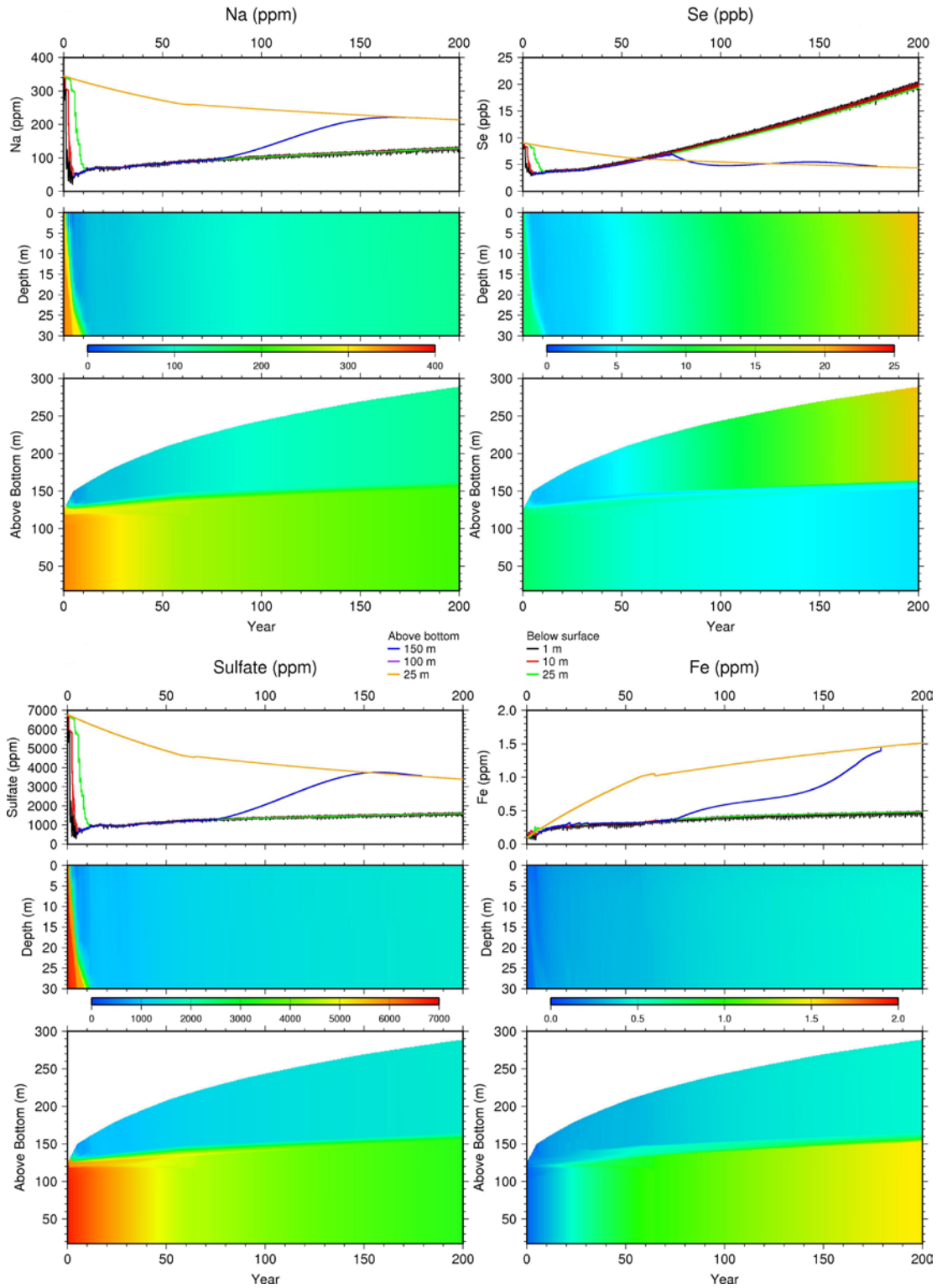

Figure 4-6: Vertical and temporal distribution of Na, Se, Sulfate, and V over 100 years from the Ajax pit lake simulation. Values are shown for the entire pit lake (bottom); upper 30 m (middle); and depths of 1, 10, and 25 m; and elevations of 25, 100, and 150 m (top)

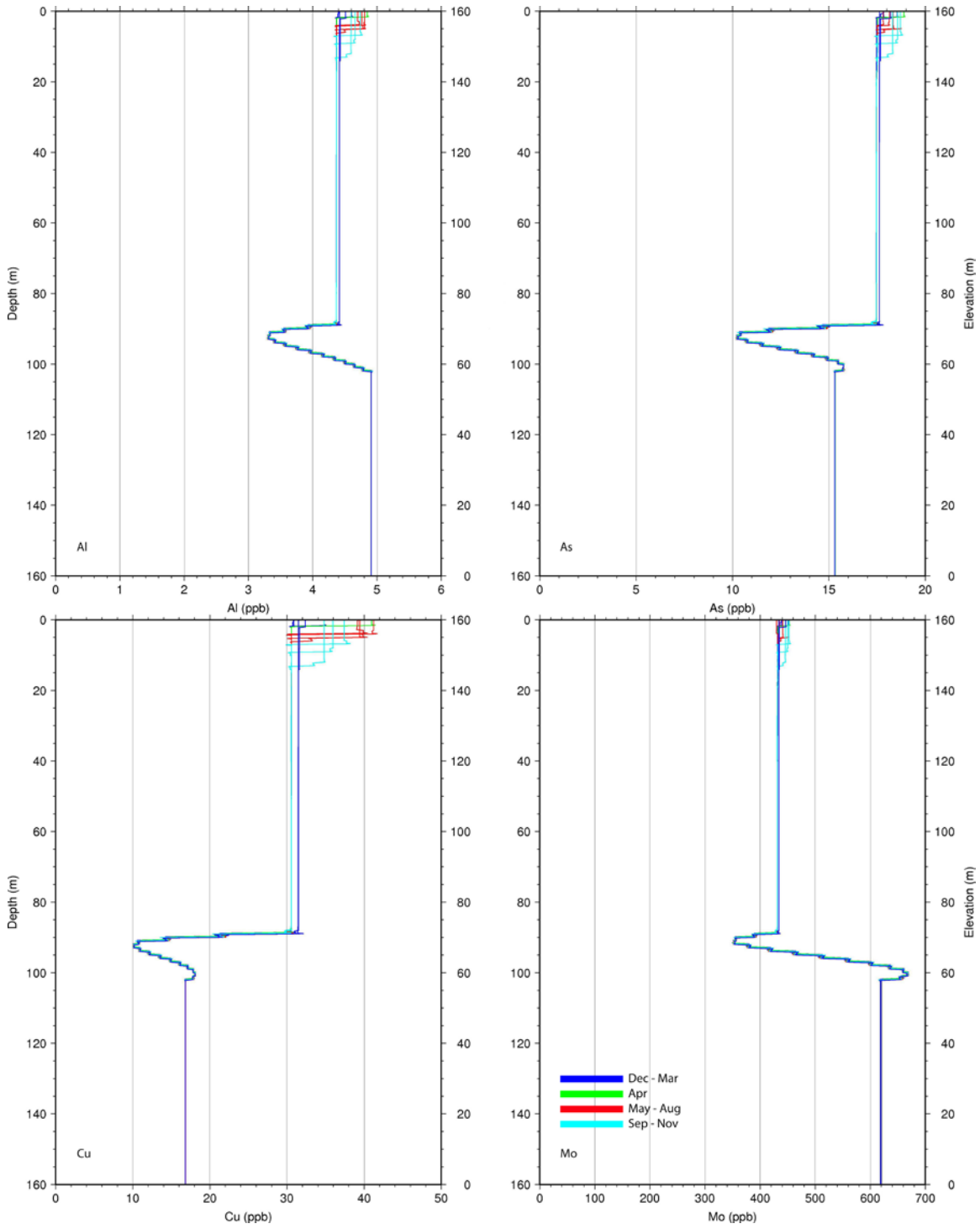

Figure 4-7: Monthly vertical profiles of Al, As, Cu and Mo during year 95 of the Ajax model simulation.

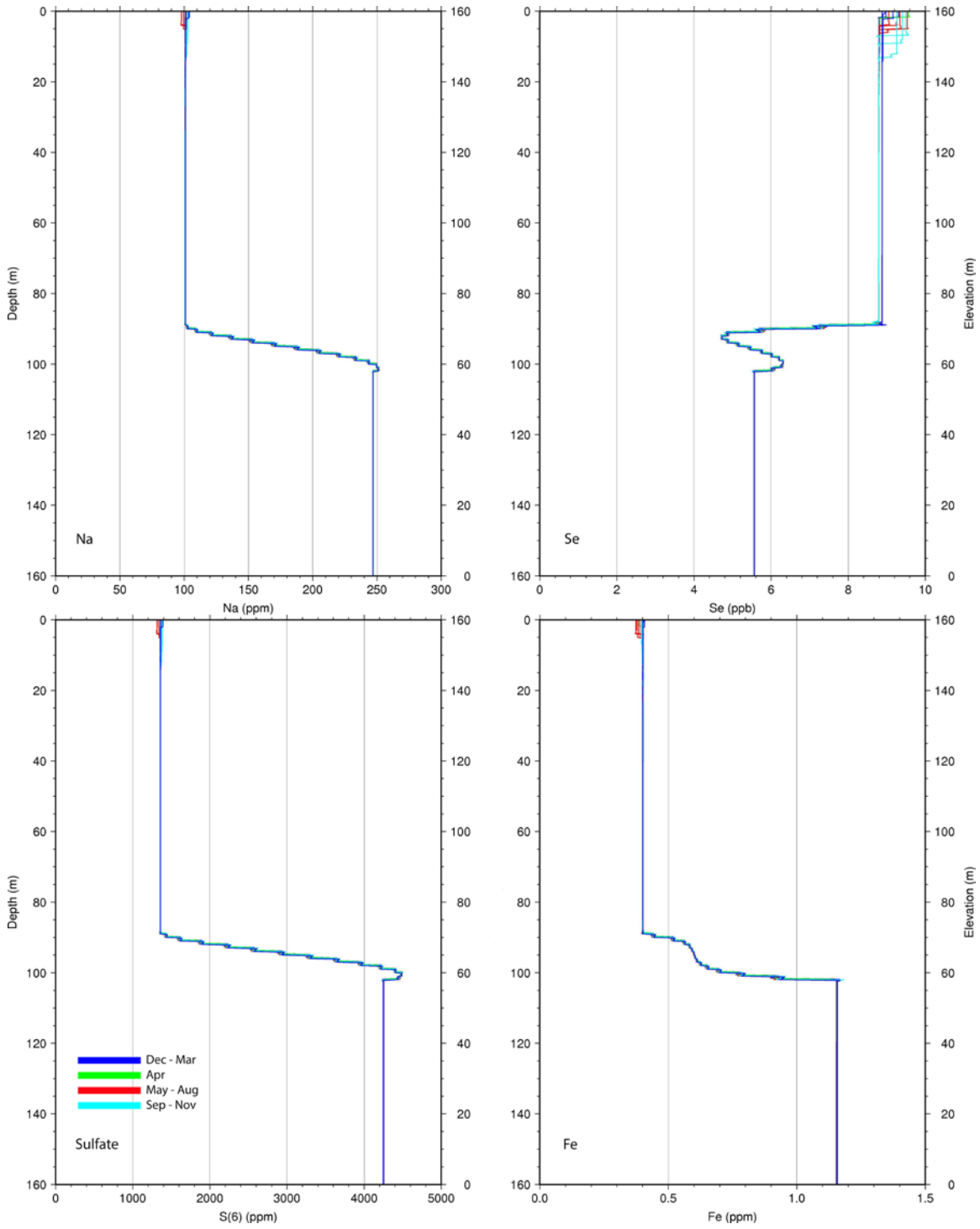

Figure 4-8: Monthly vertical profiles of Na, Se, Sulfate and Fe during year 95 of the Ajax model simulation.

5. Summary

5. Summary

A numerical model of the temporal and vertical structure of physical and chemical properties in the future Ajax pit lake over a 200-year period has been developed using the PitMod pit lake model. Inputs to the Ajax model include monthly mean values for meteorological variables, including air temperature, wind speed, relative humidity, and solar long- and short-wave radiation. Other inputs include the components of a water balance comprised of groundwater, precipitation, pit wall runoff, evaporation, surface inflows and seepage inflows from the adjacent project components. Each inflow has associated values for temperature, dissolved oxygen, pH, and concentrations for a suite of minor and major chemical species.

Pit lake morphometry is specified in the model via the prescribed relationship between elevation above the pit bottom and values for pit volume and planar surface area. Pit wall area is divided into separate regions for four different lithology types, each with its own chemical signature that is applied to the pit wall runoff. Mine rock backfill in the western lobe of the pit decreases the incremental pit lake volume and allows the pit void to fill more rapidly.

The evolution and vertical structure of the Ajax pit lake in the model are entirely dependent on the physical and chemical properties of the water balance components and on values for the meteorological inputs. In particular, the model predictions are particularly sensitive to the high density TSF Pond water and the input of relatively warm groundwater at depth. The dense high salinity TSF Pond water remains isolated in the bottom of the pit lake throughout the 200 year model simulation. This highly saline water allows the thermal structure of the simulated Ajax pit lake to contrast with a typical natural lake where bottom waters are usually at or near 4°, the temperature of maximum density of fresh water. The model predicts that a 130 m deep surface layer (epilimnion) will form with seasonal variability in temperature, salinity, DO, stability, and major species concentrations. Below this surface layer model parameters exhibit virtually no seasonal variability.

Due to minimal mixing with surface layers, the lower portions of the pit lake are predicted to become anoxic by Year 6 and remain anoxic through the balance of the 200 year simulation. The development of anoxia in the lower water column is beneficial for water quality as it is a factor contributing toward the formation of a permanent sink for metals in sediments that form in the base of the pit lake.

A relatively large chemical loading occurs during the first 4.5 years of filling via TSF surface inflow. This accounts for 14% of the total lake volume after 200 years. The TSF inflow results in elevated concentrations for most major ions, with Al, Na, and SO_4

registering their maximum near-surface concentrations within the first 5 years. Whereas other metal(oid)s have concentration increases that are produced by seepage inflows from the TSF. The chemical species that are predicted to maintain concentrations elevated above British Columbia wildlife guidelines include As, Mo and Se.

The implementation of the Ajax PitMod model in conservative mode provides a reasonable simulation but likely over estimates metal cation concentrations as it does not account for scavenging and particle settling mechanisms that are common in natural lakes. Scavenging mechanisms are most prominent in eutrophic lakes that have a high rate of biological productivity or mesotrophic lakes that show intermediate levels of primary productivity. Pit lakes tend to be oligotrophic, exhibiting low rates of in situ primary production and hence relatively low rates of metal attenuation. The level of productivity and associated attenuation processes of a lake can be enhanced through bioremediation methods such as organic additions or fertilization.

6. Closure

6. Closure

This draft report provides the final requirement for the pit lake model evaluating physical and chemical evolution of the Ajax pit lake. The report was prepared and reviewed by the Lorax technical personnel listed below.

Sincerely,

LORAX ENVIRONMENTAL SERVICES LTD.

Prepared by:

ORIGINAL SIGNED

Don Dunbar, M.Math. Ph.D.
Senior Oceanographer& Numerical Modeler

ORIGINAL SIGNED

Silvano Salvador, B.Sc.
Senior Environmental Data Analyst

Reviewed by:

ORIGINAL SIGNED

Bruce Mattson, M.Sc. P.Geo
Senior Environmental Geoscientist

References

KGHM

References

Achterberg, E., C. van den Berg, *et al*. (1997). "Speciation and cycling of trace metals in Esthwaite Water: A productive English lake with seasonal deep-water anoxia." Geochimica et Cosmochimica Acta **61**(24): 5233-5253.

Balistrieri, L., J. Murray, *et al.* (1994). "The geochemical cycling of trace elements in a biogenic meromictic lake." Geochimica et Cosmochimica Acta **58**(19): 3993-4008.

Charlton, M.N. (1980). "Hypolimnion Oxygen Consumption in Lakes: Discussion of Productivity and Morphometry Effects" Can. J. Fish. Aquat. Sci. **37**: 1531-1539.

Crusius J., Dunbar D. (2000) Predictions of pit lake water column properties using a coupled mixing and geochemical speciation model. Proceedings of the 39th Conference of CIM, Canadian Institute of Mining, Metallurgy and Petroleum. CIM, Toronto, Canada.

Crusius, J., D. Dunbar, *et al*. (2002). "Predictions of pit-lake water column properties using a coupled mixing and geochemical speciation model." TRANSACTIONS-SOCIETY FOR MINING METALLURGY AND EXPLORATION INCORPORATED **312**: 49-56.

Dilley, A. C. and D. M. O'Brien (1998). Estimating downward clear sky long-wave irradiance at the surface from screen temperature and precipitable water, Q. J. R. *Meteorol. Soc*., 124: 1391 - 1401

Dunbar D., Pieters, R., McNee, J.J. (2004) Modeling a negatively buoyant plume and related surface dissolved metal removal in the Equity MainZone Pit Lake. U.S. EPA Pit Lakes Conference. November 16-18, 2004, Reno, Nevada, USA.

Fenchel, T. and T. Blackburn (1979). Bacteria and mineral cycling, Academic press New York.

Froelich, P., G. Klinkhammer, *et al*. (1979). Erly oxidation of organic matter in pelagic sediments of the eastern equatorial Atlantic: Suboxic diagenesis." Geochim. Cosmochim. Acta **43**(10): 7.

Gammons, C. H. and T. E. Duaime (2006). "Long term changes in the limnology and geochemistry of the Berkeley pit lake, Butte, Montana." Mine Water and the Environment **25**(2): 76-85.

Green, W., T. Ferdelman, *et al.* (1989). "Metal dynamics in Lake Vanda(Wright Valley, Antarctica)." Chemical Geology **76**(1-2): 85-94.

Hamblin, P., C. Stevens, *et al.* (1999). "Simulation of vertical transport in mining pit lake." Journal of Hydraulic Engineering **125**: 1029.

Hamilton-Taylor, J. and W. Davison (1995). "Redox-driven cycling of trace elements in lakes." Physics and chemistry of lakes. Springer: 1–333.

Hustrulid, W. A. (1999) “Blasting Principles for Open Pit Mining” A.A. Balkema, p. 382.

Imerito, A. (2007). "Dynamic Reservoir Simulation Model DYRESM v4. v4.0 Science Manual."

Kempton, H., & Atkins, D. (2000). Delayed environmental impacts from mining in semi-arid climates. In Proceedings of the 5th International Conference on Acid Rock Drainage (Vol. 2, pp. 1299–1308). Denver, USA.

Lorax (2015) Ajax Geochemical Characterization Study prepared for KAM Ajax, July 17, 2015.

Martin A.J., McNee J.J., Crusius J, Pieters R., Dunbar D. (2003) Field-scale assessment of bioremediation strategies for two pit lakes using limnocorrals. In: International Conference on Acid Rock Drainage, Cairns, Australia, July 2003, pp 529-539

Müller B.Environmental Science and Technology 46 (18), pp 9964-9971.

Northcote, T. and W. Johnson (1964). "Occurrence and distribution of sea water in Sakinaw Lake, British Columbia." J. Fish. Res. Board Can. **21**: 1321-1324.

Patterson, J., P. Hamblin, *et al.* (1984). "Classification and dynamic simulation of the vertical density structure of lakes." Limnology and Oceanography: 845-861.

Rogers, C., G. Lawrence, *et al.* (1995). "Observations and numerical simulation of a shallow ice-covered midlatitude lake." Limnology and Oceanography: 374-385.

Parkhurst, D., C. Appelo, *et al*. (1999). User's guide to PHREEQC (Version 2): A computer program for speciation, batch-reaction, one-dimensional transport, and inverse geochemical calculations, US Geological Survey Washington, DC.

Patterson, J., P. Hamblin, *et al.* (1984). "Classification and dynamic simulation of the vertical density structure of lakes." Limnology and Oceanography: 845-861.

Pedersen, T., B. Mueller, *et al.* (1993). "The early diagenesis of submerged sulfide-rich mine tailings in Anderson Lake, Manitoba." Canadian Journal of Earth Sciences **30**(6): 1099-1109.

Sigg, L., C. Johnson, *et al.* (1991). "Redox conditions and alkalinity generation in a seasonally anoxic lake (Lake Greifen)." Marine Chemistry [MAR. CHEM.]. **36**(1-4).

Stumm, W. and J. Morgan (1981). "Aquatic chemistry: an introduction emphasizing chemical equilibria in natural waters." New York.

Appendix A: Water Quality of Pit Lake Inputs

		TSF Seepage (mg/L)	TSF + South MRSF Seepage (mg/L)	Jacko Lake Seepage (mg/L)	Central Pond (mg/L)	TSF Pond (mg/L)
H+	min	0	0	8.7	2.7	3.6
	10 pctile	0	0	8.9	2.7	4.8
	50 pctile	0	0	8.9	2.7	4.8
	90 pctile	0	0	9.3	2.7	4.8
	max	0	0	9.7	2.7	4.8
Hardness	min	225	1,492	349	424	88
	10 pctile	1,112	1,504	354	424	126
	50 pctile	1,495	1,506	358	424	179
	90 pctile	1,693	1,513	372	424	10,314
	max	2,882	1,554	391	424	12,299
SO4	min	194	1,427	57	346	60
	10 pctile	954	1,438	59	346	94
	50 pctile	1,400	1,440	59	346	141
	90 pctile	1,477	1,451	63	346	9,339
	max	2,469	1,486	66	346	11,136
Cl	min	14	2.4	60	24	3.1
	10 pctile	37	2.4	60	24	7.2
	50 pctile	69	2.4	61	24	15
	90 pctile	103	2.5	64	24	647
	max	185	2.7	67	24	772
F	min	0.0550	0.4631	0.2301	0.1358	0.0394
	10 pctile	0.2710	0.4666	0.2326	0.1358	0.0608
	50 pctile	0.4786	0.4670	0.2349	0.1358	0.0804
	90 pctile	0.5383	0.4697	0.2446	0.1358	1.9
	max	0.6982	0.4821	0.2550	0.1358	2.3
Br	min	0.0521	0.9905	0.1071	0.1703	0.0543
	10 pctile	0.2610	0.9981	0.1094	0.1703	0.0855
	50 pctile	0.6254	0.9990	0.1137	0.1703	0.1125
	90 pctile	0.8619	1.0	0.1209	0.1703	1.7
	max	0.9218	1.0	0.1278	0.1703	2.0
Al	min	0.00029	0.0027	0.0029	0.0017	0.000022
	10 pctile	0.0014	0.0027	0.0029	0.0017	0.00042
	50 pctile	0.0024	0.0027	0.0029	0.0017	0.0010
	90 pctile	0.0025	0.0027	0.0031	0.0017	0.0074
	max	0.0037	0.0028	0.0062	0.0017	0.0088
Sb	min	0.00061	0.0168	0.000069	0.0009	0.00012
	10 pctile	0.0031	0.0168	0.000071	0.0009	0.00019
	50 pctile	0.0075	0.0168	0.000077	0.0009	0.00028
	90 pctile	0.0105	0.0172	0.000084	0.0009	0.0269
	max	0.0113	0.0180	0.00009	0.0009	0.0320
As	min	0.0009	0.0798	0.0015	0.0034	0.00024
	10 pctile	0.0053	0.0804	0.0015	0.0034	0.00034
	50 pctile	0.0316	0.0805	0.0016	0.0034	0.00057
	90 pctile	0.0580	0.0809	0.0017	0.0034	0.0299
	max	0.0646	0.0831	0.0017	0.0034	0.0357
Ba	min	0.0029	0.0507	0.0739	0.0238	0.0072
	10 pctile	0.0147	0.0507	0.0742	0.0238	0.0101
	50 pctile	0.0363	0.0508	0.0752	0.0238	0.0207
	90 pctile	0.0507	0.0512	0.0779	0.0238	0.0767
	max	0.0544	0.0525	0.0818	0.0238	0.0915

		TSF Seepage (mg/L)	TSF + South MRSF Seepage (mg/L)	Jacko Lake Seepage (mg/L)	Central Pond (mg/L)	TSF Pond (mg/L)
Be	min	0.000026	0.00020	0.000053	0.000044	0.000053
	10 pctile	0.00013	0.00020	0.000053	0.000044	0.000053
	50 pctile	0.00029	0.00020	0.000054	0.000044	0.000053
	90 pctile	0.00039	0.00021	0.000056	0.000044	0.000053
	max	0.00041	0.00021	0.000059	0.000044	0.000053
B	min	0.0121	0.4013	0.0207	0.0249	0.0280
	10 pctile	0.0643	0.4044	0.0209	0.0249	0.0442
	50 pctile	0.2995	0.4048	0.0211	0.0249	0.0660
	90 pctile	0.5230	0.4071	0.0222	0.0249	0.5986
	max	0.5788	0.4178	0.0232	0.0249	0.7138
Cd	min	0.000012	0.00017	0.000005	0.000013	0.000035
	10 pctile	0.000061	0.00018	0.000006	0.000013	0.000035
	50 pctile	0.00022	0.00018	0.000006	0.000013	0.000035
	90 pctile	0.00036	0.00018	0.000006	0.000013	0.000035
	max	0.00040	0.00018	0.000009	0.000013	0.000035
Ca	min	80	457	85	83	14
	10 pctile	374	461	86	83	38
	50 pctile	485	462	87	83	286
	90 pctile	595	464	91	83	951
	max	1,031	477	96	83	1,134
Cr	min	0.000053	0.0064	0.00013	0.00021	0.00035
	10 pctile	0.00037	0.0064	0.00013	0.00021	0.00055
	50 pctile	0.0032	0.0064	0.00013	0.00021	0.00081
	90 pctile	0.0062	0.0065	0.00014	0.00021	0.0026
	max	0.0069	0.0066	0.00046	0.00021	0.0031
Co	min	0.00009	0.0019	0.00015	0.00036	0.00030
	10 pctile	0.00052	0.0019	0.00015	0.00036	0.00047
	50 pctile	0.0030	0.0019	0.00015	0.00036	0.00070
	90 pctile	0.0054	0.0019	0.00016	0.00036	0.0044
	max	0.0060	0.0020	0.00022	0.00036	0.0052
Cu	min	0.00086	0.0116	0.0022	0.0013	0.00074
	10 pctile	0.0046	0.0117	0.0022	0.0013	0.0012
	50 pctile	0.0214	0.0117	0.0022	0.0013	0.0015
	90 pctile	0.0373	0.0118	0.0024	0.0013	0.0386
	max	0.0412	0.0121	0.0031	0.0013	0.0460
Fe	min	0.000052	0.00034	0.0491	0.2013	0.0022
	10 pctile	0.00026	0.00034	0.0492	0.2013	0.0030
	50 pctile	0.00038	0.00034	0.0505	0.2013	0.0074
	90 pctile	0.00040	0.00034	0.0538	0.2013	0.1173
	max	0.00067	0.00035	0.0603	0.2013	0.1399
Pb	min	0.000080	0.00046	0.000027	0.000078	0.000074
	10 pctile	0.00039	0.00046	0.000027	0.000078	0.000074
	50 pctile	0.00063	0.00046	0.000027	0.000078	0.000074
	90 pctile	0.00065	0.00047	0.000030	0.000078	0.000074
	max	0.0010	0.00049	0.000071	0.000078	0.000074
Li	min	0.00086	0.0339	0.0058	0.0033	0.0025
	10 pctile	0.0046	0.0342	0.0059	0.0033	0.0039
	50 pctile	0.0231	0.0342	0.0059	0.0033	0.0056
	90 pctile	0.0409	0.0344	0.0062	0.0033	0.0457
	max	0.0453	0.0353	0.0065	0.0033	0.0545

		TSF Seepage (mg/L)	TSF + South MRSF Seepage (mg/L)	Jacko Lake Seepage (mg/L)	Central Pond (mg/L)	TSF Pond (mg/L)
Mg	min	5.8	85	41	54	7.1
	10 pctile	29	85	41	54	10
	50 pctile	65	85	41	54	14
	90 pctile	86	86	43	54	354
	max	91	88	45	54	423
Mn	min	0.0114	0.0551	0.0388	0.2689	0.0140
	10 pctile	0.0573	0.0552	0.0388	0.2689	0.0222
	50 pctile	0.1561	0.0553	0.0410	0.2689	0.0314
	90 pctile	0.2305	0.0562	0.0430	0.2689	0.5203
	max	0.2491	0.0578	0.0438	0.2689	0.6205
Hg	min	0.000007	0.00010	0.000005	0.000008	0.000002
	10 pctile	0.000036	0.00010	0.000005	0.000008	0.000004
	50 pctile	0.000066	0.00010	0.000006	0.000008	0.000005
	90 pctile	0.000077	0.00011	0.000006	0.000008	0.00032
	max	0.00009	0.00011	0.000010	0.000008	0.00039
Mo	min	0.0458	1.2	0.0031	0.0432	0.0428
	10 pctile	0.2328	1.2	0.0035	0.0432	0.0676
	50 pctile	0.7114	1.2	0.0040	0.0432	0.1009
	90 pctile	1.1	1.2	0.0044	0.0432	1.4
	max	1.2	1.3	0.0050	0.0432	1.7
Ni	min	0.00077	0.0547	0.0012	0.0020	0.00080
	10 pctile	0.0038	0.0552	0.0012	0.0020	0.0013
	50 pctile	0.0099	0.0553	0.0013	0.0020	0.0018
	90 pctile	0.0143	0.0559	0.0013	0.0020	0.0344
	max	0.0154	0.0575	0.0016	0.0020	0.0410
K	min	4.5	36	12	13	1.8
	10 pctile	22	37	12	13	2.4
	50 pctile	29	37	12	13	3.6
	90 pctile	33	37	13	13	190
	max	57	38	13	13	227
Se	min	0.00028	0.0355	0.00029	0.00085	0.0017
	10 pctile	0.0019	0.0364	0.00030	0.00085	0.0028
	50 pctile	0.0163	0.0368	0.00032	0.00085	0.0041
	90 pctile	0.0317	0.0370	0.00034	0.00085	0.0135
	max	0.0355	0.0379	0.00038	0.00085	0.0161
Si	min	0.8549	6.5	8.9	3.5	0.8109
	10 pctile	4.2	6.5	9.0	3.5	1.1
	50 pctile	6.6	6.5	9.1	3.5	2.2
	90 pctile	6.6	6.6	9.4	3.5	32
	max	11	6.8	9.7	3.5	38
Ag	min	0.000025	0.000025	0.000005	0.000019	0.000045
	10 pctile	0.000079	0.000025	0.000005	0.000019	0.000046
	50 pctile	0.00013	0.000025	0.000005	0.000019	0.000046
	90 pctile	0.00018	0.000025	0.000006	0.000019	0.000046
	max	0.00033	0.000026	0.000006	0.000019	0.000046
Na	min	10	27	37	57	7.7
	10 pctile	50	27	37	57	11
	50 pctile	88	27	37	57	16
	90 pctile	97	28	39	57	476
	max	130	31	41	57	567

		TSF Seepage (mg/L)	TSF + South MRSF Seepage (mg/L)	Jacko Lake Seepage (mg/L)	Central Pond (mg/L)	TSF Pond (mg/L)
Sr	min	0.4047	3.6	0.3936	0.6508	0.2933
	10 pctile	2.0	3.6	0.4002	0.6508	0.4629
	50 pctile	4.2	3.6	0.4047	0.6508	0.6615
	90 pctile	5.4	3.7	0.4222	0.6508	19
	max	5.7	3.8	0.4419	0.6508	22
Tl	min	0.000003	0.00024	0.000006	0.000009	0.000014
	10 pctile	0.000017	0.00024	0.000006	0.000009	0.000022
	50 pctile	0.00013	0.00024	0.000006	0.000009	0.000033
	90 pctile	0.00025	0.00025	0.000006	0.000009	0.00015
	max	0.00028	0.00025	0.000008	0.000009	0.00018
Sn	min	0.000037	0.00024	0.000054	0.000058	0.000027
	10 pctile	0.00034	0.00024	0.000054	0.000058	0.000082
	50 pctile	0.0050	0.00024	0.000055	0.000058	0.00029
	90 pctile	0.0102	0.00025	0.000059	0.000058	0.00084
	max	0.0115	0.00025	0.000071	0.000058	0.00084
U	min	0.0012	0.0061	0.0013	0.0020	0.00052
	10 pctile	0.0058	0.0061	0.0013	0.0020	0.00082
	50 pctile	0.0096	0.0061	0.0013	0.0020	0.0011
	90 pctile	0.0101	0.0062	0.0014	0.0020	0.0522
	max	0.0150	0.0064	0.0015	0.0020	0.0622
V	min	0.00059	0.1097	0.0026	0.0029	0.00041
	10 pctile	0.0044	0.1106	0.0026	0.0029	0.0014
	50 pctile	0.0438	0.1107	0.0026	0.0029	0.0041
	90 pctile	0.0863	0.1113	0.0028	0.0029	0.0080
	max	0.0969	0.1143	0.0031	0.0029	0.0096
Zn	min	0.0020	0.0302	0.0017	0.0024	0.0010
	10 pctile	0.0097	0.0302	0.0017	0.0024	0.0016
	50 pctile	0.0186	0.0303	0.0017	0.0024	0.0022
	90 pctile	0.0222	0.0308	0.0018	0.0024	0.0884
	max	0.0250	0.0314	0.0019	0.0024	0.1054
NH3	min	0	0	0.0565	0.0358	0.0012
	10 pctile	0	0	0.0565	0.0358	0.0018
	50 pctile	0	0	0.0569	0.0358	0.0045
	90 pctile	0	0.0636	0.0606	0.0358	0.0371
	max	0	0.9821	0.0654	0.0358	0.0442
NO3	min	0	0	0.0819	0.0741	0.0033
	10 pctile	0	0	0.0821	0.0741	0.0060
	50 pctile	0	0	0.0831	0.0741	0.0147
	90 pctile	0	0.5029	0.0924	0.0741	0.2341
	max	0	7.8	0.1065	0.0741	0.2792
NO2	min	0	0	0.0040	0.0042	0.00010
	10 pctile	0	0	0.0040	0.0042	0.00040
	50 pctile	0	0	0.0041	0.0042	0.0010
	90 pctile	0	0.0115	0.0043	0.0042	0.0214
	max	0	0.1791	0.0049	0.0042	0.0256
P	min	0.0168	0.0927	0.0887	0.0570	0.0042
	10 pctile	0.0832	0.0928	0.0891	0.0570	0.0042
	50 pctile	0.1559	0.0930	0.0896	0.0570	0.0042
	90 pctile	0.1840	0.0943	0.0927	0.0570	0.0042
	max	0.2141	0.0962	0.0960	0.0570	0.0042

		Undist'd Ground (mg/L)	TSF + South MRSF Seepage (mg/L)	Jacko Lake Seepage (mg/L)	Upgradient Pond Seepage (mg/L)
H+	1			8.0	8.9
	2			8.0	8.9
	3	8.1	0.000000	8.0	8.9
	4	8.3	0.000000	8.0	8.9
	5	8.3	0.000000	8.0	9.1
	6	8.4	0.000000	349	9.1
	7	8.4	0.000000	8.0	9.3
	8	8.4	0.000000	8.0	9.3
	9	8.2	0.000000	8.0	9.3
	10	8.2	0.000000	8.0	9.1
	11			8.0	9.1
	12			8.0	9.1
Hardness	1			589	3,545
	2			589	3,545
	3	429	1,419	589	3,545
	4	368	1,419	589	3,545
	5	368	1,419	589	1,950
	6	298	1,419	589	1,950
	7	298	1,419	589	2,540
	8	298	1,419	589	2,540
	9	401	1,419	589	2,540
	10	401	1,419	589	2,790
	11			589	2,790
	12			589	2,790
SO4	1			444	3,990
	2			444	3,990
	3	74	1,598	444	3,990
	4	49	1,598	444	3,990
	5	49	1,598	444	2,165
	6	23	1,598	444	2,165
	7	23	1,598	444	2,680
	8	23	1,598	444	2,680
	9	39	1,598	444	2,680
	10	39	1,598	444	3,060
	11			444	3,060
	12			444	3,060
Cl	1			13	92
	2			13	92
	3	65	20	13	92
	4	69	20	13	92
	5	69	20	13	42
	6	35	20	13	42
	7	35	20	13	49
	8	35	20	13	49
	9	50	20	13	49
	10	50	20	13	55
	11			13	55
	12			13	55

		Undist'd Ground (mg/L)	TSF + South MRSF Seepage (mg/L)	Jacko Lake Seepage (mg/L)	Upgradient Pond Seepage (mg/L)
F	1			0.3645	0.5000
	2			0.3645	0.5000
	3	0.3100	0.4675	0.3645	0.5000
	4	0.1575	0.4675	0.3645	0.5000
	5	0.1575	0.4675	0.3645	0.2000
	6	0.2200	0.4675	0.3645	0.2000
	7	0.2200	0.4675	0.3645	0.5000
	8	0.2200	0.4675	0.3645	0.5000
	9	0.2100	0.4675	0.3645	0.5000
	10	0.2100	0.4675	0.3645	0.5000
	11			0.3645	0.5000
	12			0.3645	0.5000
Br	1			0.3104	1.3
	2			0.3104	1.3
	3	0.2500	1.000000	0.3104	1.3
	4	0.1250	1.000000	0.3104	1.3
	5	0.1250	1.000000	0.3104	0.5000
	6	0.0250	1.000000	0.3104	0.5000
	7	0.0250	1.000000	0.3104	1.3
	8	0.0250	1.000000	0.3104	1.3
	9	0.2500	1.000000	0.3104	1.3
	10	0.2500	1.000000	0.3104	1.3
	11			0.3104	1.3
	12			0.3104	1.3
Al	1			0.0045	0.0025
	2			0.0045	0.0025
	3	0.0016	0.0029	0.0045	0.0025
	4	0.0033	0.0029	0.0045	0.0025
	5	0.0033	0.0029	0.0045	0.0075
	6	0.0029	0.0029	0.0045	0.0075
	7	0.0029	0.0029	0.0045	0.0025
	8	0.0029	0.0029	0.0045	0.0025
	9	0.0018	0.0029	0.0045	0.0025
	10	0.0018	0.0029	0.0045	0.0025
	11			0.0045	0.0025
	12			0.0045	0.0025
Sb	1			0.00026	0.0011
	2			0.00026	0.0011
	3	0.000050	0.0800	0.00026	0.0011
	4	0.000050	0.0800	0.00026	0.0011
	5	0.000050	0.0800	0.00026	0.00037
	6	0.000050	0.0800	0.00026	0.00037
	7	0.000050	0.0800	0.00026	0.00085
	8	0.000050	0.0800	0.00026	0.00085
	9	0.000050	0.0800	0.00026	0.00085
	10	0.000050	0.0800	0.00026	0.0013
	11			0.00026	0.0013
	12			0.00026	0.0013

		Undist'd Ground (mg/L)	TSF + South MRSF Seepage (mg/L)	Jacko Lake Seepage (mg/L)	Upgradient Pond Seepage (mg/L)
As	1			0.0058	0.0169
	2			0.0058	0.0169
	3	0.0014	0.0805	0.0058	0.0169
	4	0.0010	0.0805	0.0058	0.0169
	5	0.0010	0.0805	0.0058	0.0079
	6	0.0017	0.0805	0.0058	0.0079
	7	0.0017	0.0805	0.0058	0.0115
	8	0.0017	0.0805	0.0058	0.0115
	9	0.0012	0.0805	0.0058	0.0115
	10	0.0012	0.0805	0.0058	0.0151
	11			0.0058	0.0151
	12			0.0058	0.0151
Ba	1			0.0627	0.0411
	2			0.0627	0.0411
	3	0.0781	0.0411	0.0627	0.0411
	4	0.0791	0.0411	0.0627	0.0411
	5	0.0791	0.0411	0.0627	0.0437
	6	0.0653	0.0411	0.0627	0.0437
	7	0.0653	0.0411	0.0627	0.0398
	8	0.0653	0.0411	0.0627	0.0398
	9	0.0918	0.0411	0.0627	0.0398
	10	0.0918	0.0411	0.0627	0.0325
	11			0.0627	0.0325
	12			0.0627	0.0325
Be	1			0.000050	0.00025
	2			0.000050	0.00025
	3	0.000050	0.00023	0.000050	0.00025
	4	0.000050	0.00023	0.000050	0.00025
	5	0.000050	0.00023	0.000050	0.00018
	6	0.000050	0.00023	0.000050	0.00018
	7	0.000050	0.00023	0.000050	0.00025
	8	0.000050	0.00023	0.000050	0.00025
	9	0.000050	0.00023	0.000050	0.00025
	10	0.000050	0.00023	0.000050	0.00025
	11			0.000050	0.00025
	12			0.000050	0.00025
B	1			0.0497	0.0250
	2			0.0497	0.0250
	3	0.0085	0.4052	0.0497	0.0250
	4	0.0050	0.4052	0.0497	0.0250
	5	0.0050	0.4052	0.0497	0.0270
	6	0.0150	0.4052	0.0497	0.0270
	7	0.0150	0.4052	0.0497	0.0250
	8	0.0150	0.4052	0.0497	0.0250
	9	0.0135	0.4052	0.0497	0.0250
	10	0.0135	0.4052	0.0497	0.0250
	11			0.0497	0.0250
	12			0.0497	0.0250

		Undist'd Ground (mg/L)	TSF + South MRSF Seepage (mg/L)	Jacko Lake Seepage (mg/L)	Upgradient Pond Seepage (mg/L)
Cd	1			0.000012	0.000025
	2			0.000012	0.000025
	3	0.000005	0.00045	0.000012	0.000025
	4	0.000005	0.00045	0.000012	0.000025
	5	0.000005	0.00045	0.000012	0.000018
	6	0.000005	0.00045	0.000012	0.000018
	7	0.000005	0.00045	0.000012	0.000025
	8	0.000005	0.00045	0.000012	0.000025
	9	0.000005	0.00045	0.000012	0.000025
	10	0.000005	0.00045	0.000012	0.000025
	11			0.000012	0.000025
	12			0.000012	0.000025
Ca	1			87	30
	2			87	30
	3	99	450	87	30
	4	95	450	87	30
	5	95	450	87	24
	6	67	450	87	24
	7	67	450	87	33
	8	67	450	87	33
	9	99	450	87	33
	10	99	450	87	25
	11			87	25
	12			87	25
Cr	1			0.00028	0.00025
	2			0.00028	0.00025
	3	0.00014	0.0066	0.00028	0.00025
	4	0.00013	0.0066	0.00028	0.00025
	5	0.00013	0.0066	0.00028	0.00018
	6	0.00011	0.0066	0.00028	0.00018
	7	0.00011	0.0066	0.00028	0.00025
	8	0.00011	0.0066	0.00028	0.00025
	9	0.00016	0.0066	0.00028	0.00025
	10	0.00016	0.0066	0.00028	0.00025
	11			0.00028	0.00025
	12			0.00028	0.00025
Co	1			0.0032	0.00025
	2			0.0032	0.00025
	3	0.00032	0.0063	0.0032	0.00025
	4	0.00011	0.0063	0.0032	0.00025
	5	0.00011	0.0063	0.0032	0.00023
	6	0.00013	0.0063	0.0032	0.00023
	7	0.00013	0.0063	0.0032	0.00025
	8	0.00013	0.0063	0.0032	0.00025
	9	0.00024	0.0063	0.0032	0.00025
	10	0.00024	0.0063	0.0032	0.00025
	11			0.0032	0.00025
	12			0.0032	0.00025

		Undist'd Ground (mg/L)	TSF + South MRSF Seepage (mg/L)	Jacko Lake Seepage (mg/L)	Upgradient Pond Seepage (mg/L)
Cu	1			0.00025	0.00050
	2			0.00025	0.00050
	3	0.0016	0.0116	0.00025	0.00050
	4	0.0024	0.0116	0.00025	0.00050
	5	0.0024	0.0116	0.00025	0.0018
	6	0.0022	0.0116	0.00025	0.0018
	7	0.0022	0.0116	0.00025	0.0011
	8	0.0022	0.0116	0.00025	0.0011
	9	0.0012	0.0116	0.00025	0.0011
	10	0.0012	0.0116	0.00025	0.00050
	11			0.00025	0.00050
	12			0.00025	0.00050
Fe	1			2.8	0.0100
	2			2.8	0.0100
	3	0.1090	0.00032	2.8	0.0100
	4	0.0375	0.00032	2.8	0.0100
	5	0.0375	0.00032	2.8	0.0100
	6	0.0470	0.00032	2.8	0.0100
	7	0.0470	0.00032	2.8	0.0100
	8	0.0470	0.00032	2.8	0.0100
	9	0.0635	0.00032	2.8	0.0100
	10	0.0635	0.00032	2.8	0.0150
	11			2.8	0.0150
	12			2.8	0.0150
Pb	1			0.000057	0.00013
	2			0.000057	0.00013
	3	0.000025	0.00064	0.000057	0.00013
	4	0.000025	0.00064	0.000057	0.00013
	5	0.000025	0.00064	0.000057	0.000088
	6	0.000025	0.00064	0.000057	0.000088
	7	0.000025	0.00064	0.000057	0.00013
	8	0.000025	0.00064	0.000057	0.00013
	9	0.000025	0.00064	0.000057	0.00013
	10	0.000025	0.00064	0.000057	0.00013
	11			0.000057	0.00013
	12			0.000057	0.00013
Li	1			0.0102	0.0050
	2			0.0102	0.0050
	3	0.0049	0.0343	0.0102	0.0050
	4	0.0035	0.0343	0.0102	0.0050
	5	0.0035	0.0343	0.0102	0.0024
	6	0.0039	0.0343	0.0102	0.0024
	7	0.0039	0.0343	0.0102	0.0029
	8	0.0039	0.0343	0.0102	0.0029
	9	0.0054	0.0343	0.0102	0.0029
	10	0.0054	0.0343	0.0102	0.0038
	11			0.0102	0.0038
	12			0.0102	0.0038

		Undist'd Ground (mg/L)	TSF + South MRSF Seepage (mg/L)	Jacko Lake Seepage (mg/L)	Upgradient Pond Seepage (mg/L)
Mg	1			89	843
	2			89	843
	3	45	72	89	843
	4	30	72	89	843
	5	30	72	89	456
	6	29	72	89	456
	7	29	72	89	586
	8	29	72	89	586
	9	37	72	89	586
	10	37	72	89	664
	11			89	664
	12			89	664
Mn	1			3.5	0.1125
	2			3.5	0.1125
	3	0.0975	0.1892	3.5	0.1125
	4	0.0257	0.1892	3.5	0.1125
	5	0.0257	0.1892	3.5	0.0916
	6	0.0269	0.1892	3.5	0.0916
	7	0.0269	0.1892	3.5	0.0299
	8	0.0269	0.1892	3.5	0.0299
	9	0.1195	0.1892	3.5	0.0299
	10	0.1195	0.1892	3.5	0.0879
	11			3.5	0.0879
	12			3.5	0.0879
Hg	1			0.000005	0.000005
	2			0.000005	0.000005
	3	0.000005	0.00019	0.000005	0.000005
	4	0.000005	0.00019	0.000005	0.000005
	5	0.000005	0.00019	0.000005	0.000005
	6	0.000005	0.00019	0.000005	0.000005
	7	0.000005	0.00019	0.000005	0.000005
	8	0.000005	0.00019	0.000005	0.000005
	9	0.000005	0.00019	0.000005	0.000005
	10	0.000005	0.00019	0.000005	0.000005
	11			0.000005	0.000005
	12			0.000005	0.000005
Mo	1			0.0294	0.0167
	2			0.0294	0.0167
	3	0.0026	1.5	0.0294	0.0167
	4	0.0021	1.5	0.0294	0.0167
	5	0.0021	1.5	0.0294	0.0173
	6	0.0021	1.5	0.0294	0.0173
	7	0.0021	1.5	0.0294	0.0175
	8	0.0021	1.5	0.0294	0.0175
	9	0.0025	1.5	0.0294	0.0175
	10	0.0025	1.5	0.0294	0.0209
	11			0.0294	0.0209
	12			0.0294	0.0209

		Undist'd Ground (mg/L)	TSF + South MRSF Seepage (mg/L)	Jacko Lake Seepage (mg/L)	Upgradient Pond Seepage (mg/L)
Ni	1			0.0051	0.0013
	2			0.0051	0.0013
	3	0.0015	0.1916	0.0051	0.0013
	4	0.0009	0.1916	0.0051	0.0013
	5	0.0009	0.1916	0.0051	0.0011
	6	0.0012	0.1916	0.0051	0.0011
	7	0.0012	0.1916	0.0051	0.0013
	8	0.0012	0.1916	0.0051	0.0013
	9	0.0023	0.1916	0.0051	0.0013
	10	0.0023	0.1916	0.0051	0.0013
	11			0.0051	0.0013
	12			0.0051	0.0013
K	1			10.0	145
	2			10.0	145
	3	13	35	10.0	145
	4	8.5	35	10.0	145
	5	8.5	35	10.0	79
	6	8.6	35	10.0	79
	7	8.6	35	10.0	105
	8	8.6	35	10.0	105
	9	12	35	10.0	105
	10	12	35	10.0	122
	11			10.0	122
	12			10.0	122
Se	1			0.00022	0.0012
	2			0.00022	0.0012
	3	0.00028	0.0800	0.00022	0.0012
	4	0.00034	0.0800	0.00022	0.0012
	5	0.00034	0.0800	0.00022	0.0012
	6	0.00018	0.0800	0.00022	0.0012
	7	0.00018	0.0800	0.00022	0.0010
	8	0.00018	0.0800	0.00022	0.0010
	9	0.00015	0.0800	0.00022	0.0010
	10	0.00015	0.0800	0.00022	0.0009
	11			0.00022	0.0009
	12			0.00022	0.0009
Si	1			12	7.4
	2			12	7.4
	3	9.5	6.6	12	7.4
	4	8.1	6.6	12	7.4
	5	8.1	6.6	12	3.6
	6	9.7	6.6	12	3.6
	7	9.7	6.6	12	4.3
	8	9.7	6.6	12	4.3
	9	11	6.6	12	4.3
	10	11	6.6	12	4.9
	11			12	4.9
	12			12	4.9

		Undist'd Ground (mg/L)	TSF + South MRSF Seepage (mg/L)	Jacko Lake Seepage (mg/L)	Upgradient Pond Seepage (mg/L)
Ag	1			0.000006	0.000025
	2			0.000006	0.000025
	3	0.000005	0.000025	0.000006	0.000025
	4	0.000005	0.000025	0.000006	0.000025
	5	0.000005	0.000025	0.000006	0.000018
	6	0.000005	0.000025	0.000006	0.000018
	7	0.000005	0.000025	0.000006	0.000025
	8	0.000005	0.000025	0.000006	0.000025
	9	0.000005	0.000025	0.000006	0.000025
	10	0.000005	0.000025	0.000006	0.000025
	11			0.000006	0.000025
	12			0.000006	0.000025
Na	1			101	861
	2			101	861
	3	37	160	101	861
	4	35	160	101	861
	5	35	160	101	463
	6	26	160	101	463
	7	26	160	101	588
	8	26	160	101	588
	9	34	160	101	588
	10	34	160	101	696
	11			101	696
	12			101	696
Sr	1			0.6457	5.0
	2			0.6457	5.0
	3	0.4710	3.6	0.6457	5.0
	4	0.3765	3.6	0.6457	5.0
	5	0.3765	3.6	0.6457	2.7
	6	0.3085	3.6	0.6457	2.7
	7	0.3085	3.6	0.6457	3.4
	8	0.3085	3.6	0.6457	3.4
	9	0.4190	3.6	0.6457	3.4
	10	0.4190	3.6	0.6457	3.9
	11			0.6457	3.9
	12			0.6457	3.9
Tl	1			0.000018	0.000025
	2			0.000018	0.000025
	3	0.000005	0.00025	0.000018	0.000025
	4	0.000005	0.00025	0.000018	0.000025
	5	0.000005	0.00025	0.000018	0.000018
	6	0.000005	0.00025	0.000018	0.000018
	7	0.000005	0.00025	0.000018	0.000025
	8	0.000005	0.00025	0.000018	0.000025
	9	0.000005	0.00025	0.000018	0.000025
	10	0.000005	0.00025	0.000018	0.000025
	11			0.000018	0.000025
	12			0.000018	0.000025

		Undist'd Ground (mg/L)	TSF + South MRSF Seepage (mg/L)	Jacko Lake Seepage (mg/L)	Upgradient Pond Seepage (mg/L)
Sn	1			0.00010	0.00025
	2			0.00010	0.00025
	3	0.000050	0.00025	0.00010	0.00025
	4	0.000050	0.00025	0.00010	0.00025
	5	0.000050	0.00025	0.00010	0.00018
	6	0.000050	0.00025	0.00010	0.00018
	7	0.000050	0.00025	0.00010	0.00025
	8	0.000050	0.00025	0.00010	0.00025
	9	0.000050	0.00025	0.00010	0.00025
	10	0.000050	0.00025	0.00010	0.00025
	11			0.00010	0.00025
	12			0.00010	0.00025
U	1			0.0090	0.0065
	2			0.0090	0.0065
	3	0.0023	0.0146	0.0090	0.0065
	4	0.0014	0.0146	0.0090	0.0065
	5	0.0014	0.0146	0.0090	0.0046
	6	0.00077	0.0146	0.0090	0.0046
	7	0.00077	0.0146	0.0090	0.0051
	8	0.00077	0.0146	0.0090	0.0051
	9	0.0011	0.0146	0.0090	0.0051
	10	0.0011	0.0146	0.0090	0.0056
	11			0.0090	0.0056
	12			0.0090	0.0056
V	1			0.00050	0.0025
	2			0.00050	0.0025
	3	0.0026	0.1108	0.00050	0.0025
	4	0.0025	0.1108	0.00050	0.0025
	5	0.0025	0.1108	0.00050	0.0028
	6	0.0029	0.1108	0.00050	0.0028
	7	0.0029	0.1108	0.00050	0.0025
	8	0.0029	0.1108	0.00050	0.0025
	9	0.0016	0.1108	0.00050	0.0025
	10	0.0016	0.1108	0.00050	0.0025
	11			0.00050	0.0025
	12			0.00050	0.0025
Zn	1			0.0038	0.0025
	2			0.0038	0.0025
	3	0.0019	0.0644	0.0038	0.0025
	4	0.0015	0.0644	0.0038	0.0025
	5	0.0015	0.0644	0.0038	0.0044
	6	0.0012	0.0644	0.0038	0.0044
	7	0.0012	0.0644	0.0038	0.0025
	8	0.0012	0.0644	0.0038	0.0025
	9	0.0019	0.0644	0.0038	0.0025
	10	0.0019	0.0644	0.0038	0.0025
	11			0.0038	0.0025
	12			0.0038	0.0025

		Undist'd Ground (mg/L)	**TSF + South MRSF Seepage (mg/L)**	**Jacko Lake Seepage (mg/L)**	**Upgradient Pond Seepage (mg/L)**
NH3	1			0.0868	3.2
	2			0.0868	3.2
	3	0.0598	0.000000	0.0868	3.2
	4	0.0228	0.000000	0.0868	3.2
	5	0.0228	0.000000	0.0868	0.2197
	6	0.0196	0.000000	0.0868	0.2197
	7	0.0196	0.000000	0.0868	0.0883
	8	0.0196	0.000000	0.0868	0.0883
	9	0.0196	0.000000	0.0868	0.0883
	10	0.0196	0.000000	0.0868	0.1360
	11			0.0868	0.1360
	12			0.0868	0.1360
NO3	1			0.0392	0.2325
	2			0.0392	0.2325
	3	0.1680	0.000000	0.0392	0.2325
	4	0.0744	0.000000	0.0392	0.2325
	5	0.0744	0.000000	0.0392	0.0500
	6	0.0559	0.000000	0.0392	0.0500
	7	0.0559	0.000000	0.0392	0.1250
	8	0.0559	0.000000	0.0392	0.1250
	9	0.0250	0.000000	0.0392	0.1250
	10	0.0250	0.000000	0.0392	0.1250
	11			0.0392	0.1250
	12			0.0392	0.1250
NO2	1			0.0082	0.0250
	2			0.0082	0.0250
	3	0.0050	0.000000	0.0082	0.0250
	4	0.0050	0.000000	0.0082	0.0250
	5	0.0050	0.000000	0.0082	0.0100
	6	0.0014	0.000000	0.0082	0.0100
	7	0.0014	0.000000	0.0082	0.0250
	8	0.0014	0.000000	0.0082	0.0250
	9	0.0050	0.000000	0.0082	0.0250
	10	0.0050	0.000000	0.0082	0.0250
	11			0.0082	0.0250
	12			0.0082	0.0250
P	1			0.0295	0.9135
	2			0.0295	0.9135
	3	0.0898	0.2198	0.0295	0.9135
	4	0.0636	0.2198	0.0295	0.9135
	5	0.0636	0.2198	0.0295	0.5060
	6	0.1145	0.2198	0.0295	0.5060
	7	0.1145	0.2198	0.0295	0.4080
	8	0.1145	0.2198	0.0295	0.4080
	9	0.0659	0.2198	0.0295	0.4080
	10	0.0659	0.2198	0.0295	0.4380
	11			0.0295	0.4380
	12			0.0295	0.4380